Master's Thesis

Post-transcriptional mechanisms underlying ATAXIN-2 dependent gene expression in *Drosophila*

Eunseok Yoo

Department of Biological Sciences

Graduate School of UNIST

2017

Post-transcriptional mechanisms underlying ATAXIN-2 dependent gene expression in *Drosophila*

Eunseok Yoo

Department of Biological Sciences

Graduate School of UNIST

Post-transcriptional mechanisms underlying ATAXIN-2 dependent gene expression in *Drosophila*

A thesis/dissertation
submitted to the Graduate School of UNIST
in partial fulfillment of the
requirements for the degree of
Master of Science

Eunseok Yoo

6/ 29/ 2017 of submission

Approved by

Advisor
Chunghun Lim

Post-transcriptional mechanisms underlying ATAXIN-2 dependent gene expression in *Drosophila*

Eunseok Yoo

This certifies that the thesis/dissertation of Eunseok Yoo is approved.

6/ 29/ 2017 of submission

signature

Advisor: Chunghun Lim

signature

Chunghun Lim: Thesis Committee Member #1

signature

Myunggon Ko: Thesis Committee Member #2

signature

Eunhee Kim: Thesis Committee Member #3

Abstract

ATAXIN-2 (ATX2) is a RNA-binding protein that regulates gene expression at post-transcriptional levels. However, it is largely unknown what other factors contribute to ATX2-dependent gene regulation and how ATX2 controls the translation of its associating mRNAs. Here, I found two ATX2-interacting factors, LSM12 and ME31B, which play their distinct roles in post-transcriptional regulatory mechanisms in *Drosophila* circadian pacemaker neurons. LSM12 acts as an adaptor of the ATX2-associating protein complex to recruit TYF. The activator complex, ATX2-LSM12-TYF, associates with 5' cap-binding translation initiation factors in an ATX2-dependent manner, thereby supporting TYF-dependent translational activation. On the other hand, a translational repressor/decapping activator ME31B/DDX6 facilitates the association of ATX2 with NOT1, a scaffold protein of CCR4-NOT deadenylase complex. The repressor complex, ATX2-ME31B-NOT1, contributes to NOT1-dependent gene silencing on selective mRNAs with short poly(A)-tails. These two opposing post-transcriptional regulator complexes govern circadian periodicity and rhythms amplitude, respectively, to sustain robust, 24-hour locomotor rhythms. To obtain additional insights for ATX2-dependent gene expression, I examined the post-transcriptional activity of RNA-tethered ATX2 on a series of RNA reporters. ATX2 tethering to 3' end of reporter transcripts activates the reporter expression in a manner dependent on poly(A)-binding protein (PABP)-interacting motif (PAM2). The translational activation by ATX2 is most evident in poly(A) tail-deficient and non-circularized reporter transcripts. Inclusion of a poly(A)-track in the reporter or RNA interference (RNAi)-mediated depletion of PABP weakens the translational activation by ATX2. By contrast, ATX2 tethering to the 5' end of reporter transcripts represses its translation in a PAM2-independent manner. Finally, ATX2 has no effects on internal ribosomal entry sites (IRES)-mediated translation, suggesting that ATX2 specifically activates cap-dependent translation. Taken together, these data demonstrate that 1) ATX2 employs a specific factor to exhibit its post-transcriptional effects and sustain circadian locomotor rhythms in *Drosophila*; and 2) ATX2-PABP interaction might support mRNA circularization particularly in poly(A)-deficient transcripts to stimulate translational initiation by ribosome recycling given that PABP directly binds to the 5' cap-binding translation initiation factor, eIF4G.

Key words: ATAXIN-2 (ATX2), RNA-binding protein, post-transcriptional regulation, cap-dependent translation, circadian clock, drosophila

Contents

Part 2. Roles of ATX2 on mRNA translation in *Drosophila* S2 cell

List of figures

Abbreviations

mRNA : messenger RNA

snRNPs : small nuclear ribonucleoproteins

m^7G : 7-methylguanosine

eIF2 : eukaryotic initiation factor 2

RBP : RNA-binding protein

RNP : ribonucleoprotein

PABP : poly (A)- binding protein

PAM2 : PABP – interacting motif

polyQ : polyglutamine

SCA2 : spinocerebellar ataxia type2

ALS : amyotrophic lateral sclerosis

UTR : untranslated region

RNAi : RNA interference

IP : immunoprecipitation

FLUC : *Firefly* luciferase

Rluc : *Renilla* luciferase

miRNA : microRNA

SD : silencing domain

SV40 : Simian virus 40

HhR : hammerhead ribozyme

HSL : histone stem-loop

ORF : open reading frame

CrPV : Cricket Paralysis Virus

IRES : internal ribosomal entry sites

GSH : glutathione

I. Introduction

I-1. Post-transcriptional regulation of gene expression

Gene expression is the process converting genetic information into functional products controlled at various levels including transcription and translation (**Figure I-1**). A gene is a segment of DNA within the genome including codes for protein synthesis. It contains exons of expressed sequences (blue, **Figure I-1**) and introns of intervening sequences (green, **Figure I-1**). Transcription produces single-stranded RNA, called messenger RNA (mRNA), from double-stranded DNA in nucleus. The mRNA maturates through RNA splicing that is one of RNA processing removing introns (green, **Figure I-1**) and linking distant exons (red, **Figure I-1**) by specific small nuclear ribonucleoproteins (snRNPs). Spliced mRNAs go through 5' capping (pink sphere, **Figure I-1**) and 3' polyadenylation (AAAA, **Figure I-1**). 5' capping is the process which a 7-methylguanosine (m^7G) cap is added to the 5' end of mRNA to promote ribosome binding and protect mRNA from degradation. 3' polyadenylation is the addition of a poly A tail to the 3' end to affect nuclear export, translation, and mRNA stability. The completed mRNA in RNA processing (mature mRNA) is exported to cytoplasm and it is finally prepared for translation. The mature RNA is translated into protein in cytoplasm by ribosome and recruiting proteins.

Post-transcriptional regulation refers to the control of gene expression at RNA levels concerning the process of translation. In particular, these translational regulation is essential to maintain protein homeostasis, called proteostasis, in diverse cellular environment. Translation is initiated by ribosome recruiting via 43S pre-initiation complex and cap-binding complex (**Figure I-2**) [1, 2]. GTP-bound eIF2 (eukaryotic initiation factor 2) associates with methionyl-transfer RNA (Met-$tRNA_i^{Met}$) and 40S ribosomal subunit. With additional initiation factors, eIF3 and eIF1A, they form 43S pre-initiation complex. Cap-binding complex is composed of eIF4E, eIF4G, and eIF4A. A cap-binding protein, eIF4E, recognizes m^7G of 5' RNA and binds to eIF4G that is a scaffold protein for direct binding of each factors. eIF4A is a ATP-dependent helicase. The eIF4G also could directly interact with eIF3 and recruit the 43S pre-initiation complex to the mRNA. Then, 60S ribosomal subunit is assembled and 80S ribosome is build. The ribosome initiates scanning from the 5' end of mRNA to the start codon, AUG, and the translation occurs. In eukaryotes, translation initiation is a rate-limiting step for the expression [3]. Thus, post-transcriptional gene regulation at RNA levels is significant to modulate the event. RNA-binding proteins (RBPs) have at least one RNA-binding domain allowing RNA interaction to form ribonucleoprotein (RNP) complexes [4, 5]. RBPs regulate

RNA fates and functions including biogenesis, stability, and cellular localization. One of RBPs, poly A binding protein (PABP) in 3' of RNA directly interacts with eIF4G in 5' making a closed-loop in the transcript probably to promote translational initiation by ribosome recycling (**Figure I-2**) [2, 6-9]. It indicates not only RNA processing such as 5' capping and polyadenylation but RBPs are also important for the translational controls.

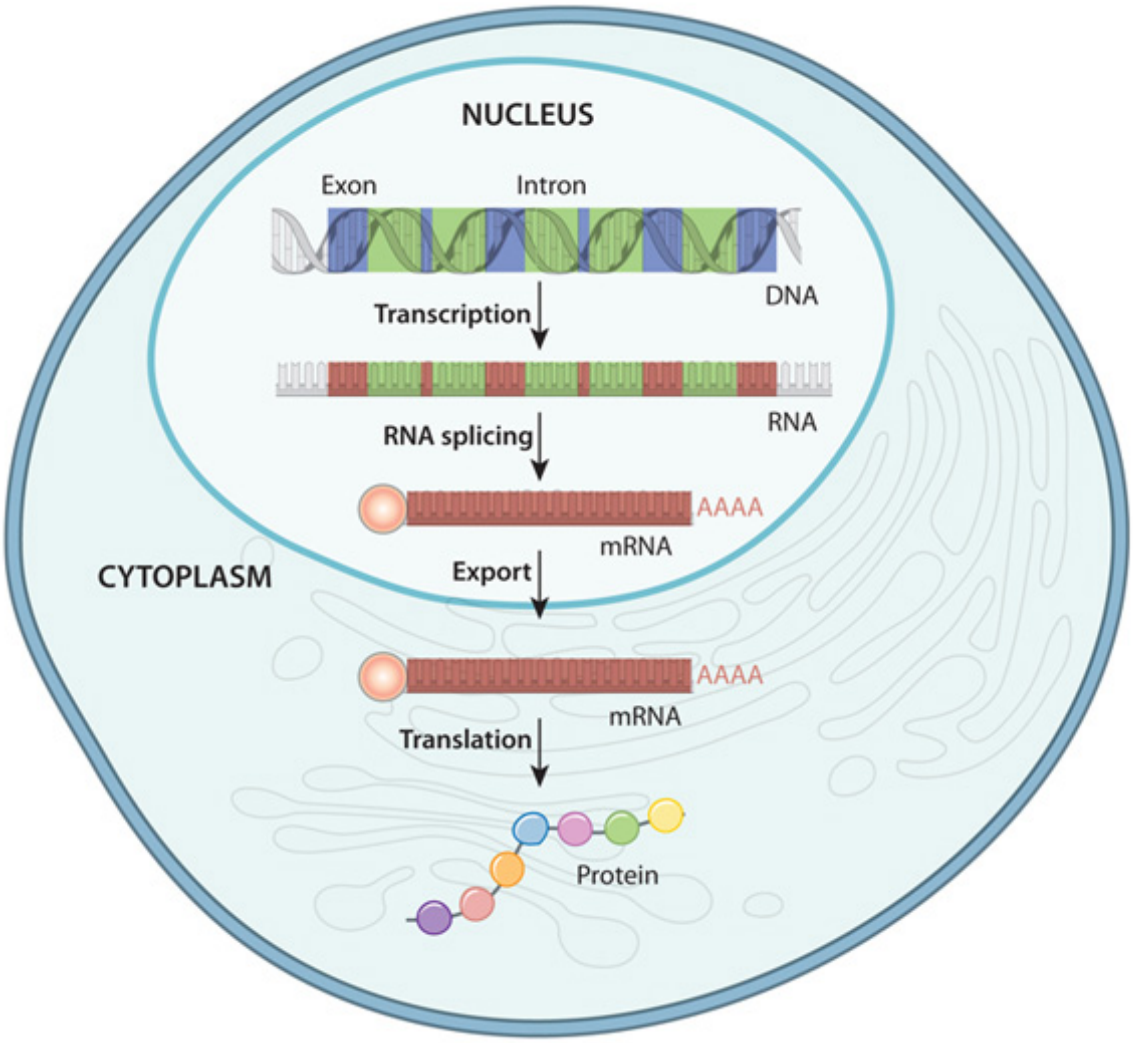

Figure I-1. Gene expression in Eukaryotes

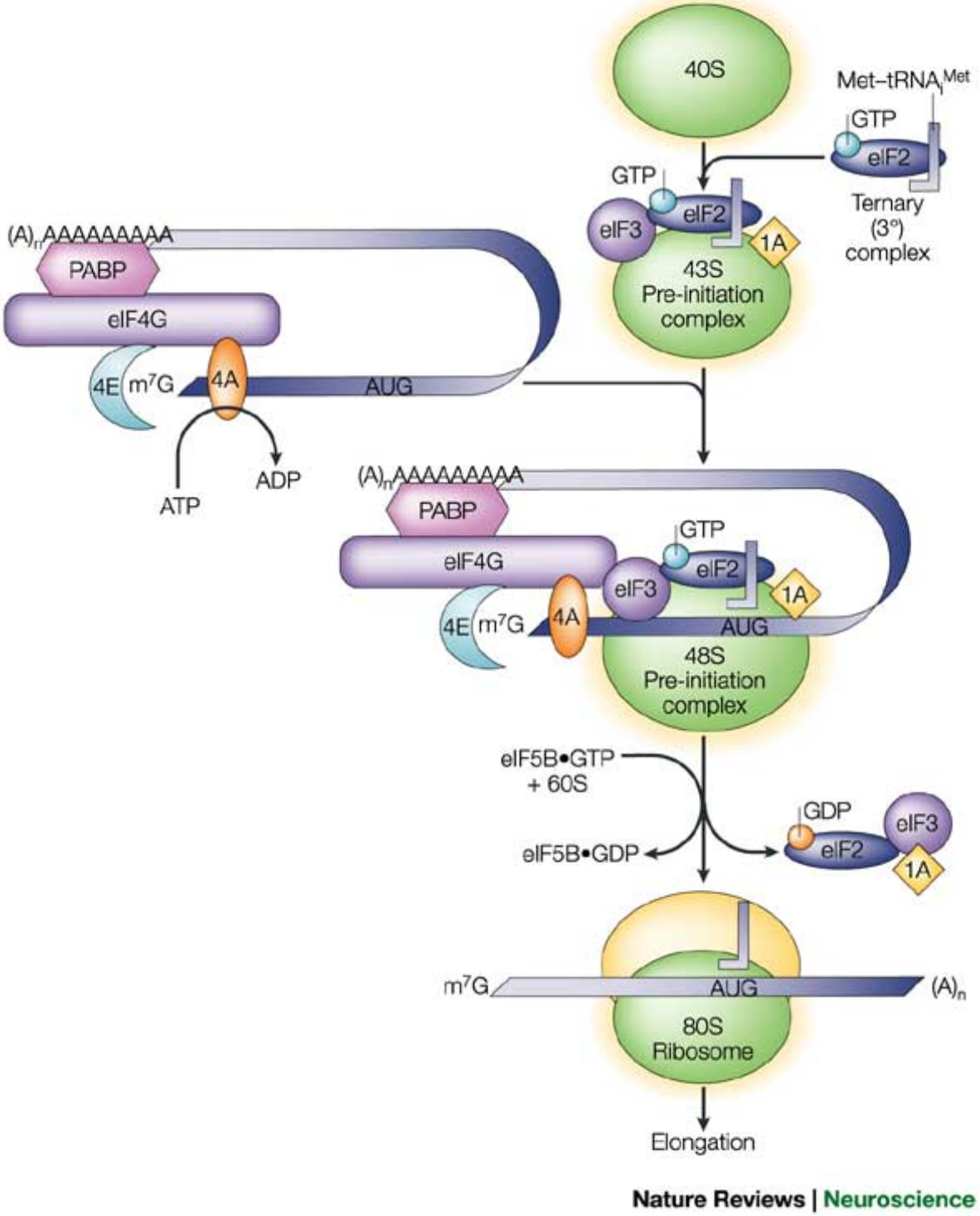

Figure I-2. The mechanism of eukaryotic translation initiation **[2]**

I-2. Circadian clock

Circadian clocks are internal molecular oscillators in organisms with 24-hour periodicity to adapt to cyclic surroundings. It is conserved from plants to human to present its physiological functions and behaviors. Many biological processes are regulated including sleep, locomotor activity (**Figure I-3**), core body temperature, hormone production, and cell cycling [10]. Conserved transcriptional feedback loops play an important role in eukaryotic circadian clock to maintain the rhythmicity at the molecular level. In *Drosophila*, the transcription factors, CLOCK (CLK)- CYCLE (CYC) dimer induces the transcription of core clock genes including *period* (*per*), *timeless* (*tim*), *vrille* (*vri*), *PAR domain protein 1* (*Pdp1*) and *clockwork orange* (*cwo*) (**Figure I-4)** [10]. These products, PER and TIM proteins form a heterodimer that represses its transcription with negative feedback by blocking the transcriptional activity of CLK-CYC. TIM is degraded in response to light by interaction with an intracellular photoreceptor, cryptochrome (CRY) [11]. The TIM degradation triggers exposure of PER to double-time (DBT) for phosphorylation and subsequent proteasomal degradation [12]. Thus, the activity of CLK-CYC dimer is de-repressed and it resets the transcriptional cycle of core clock genes (**Figure I-5**) [13]. The oscillation of mRNA abundance by cyclic transcriptional regulation brings various physiological outputs.

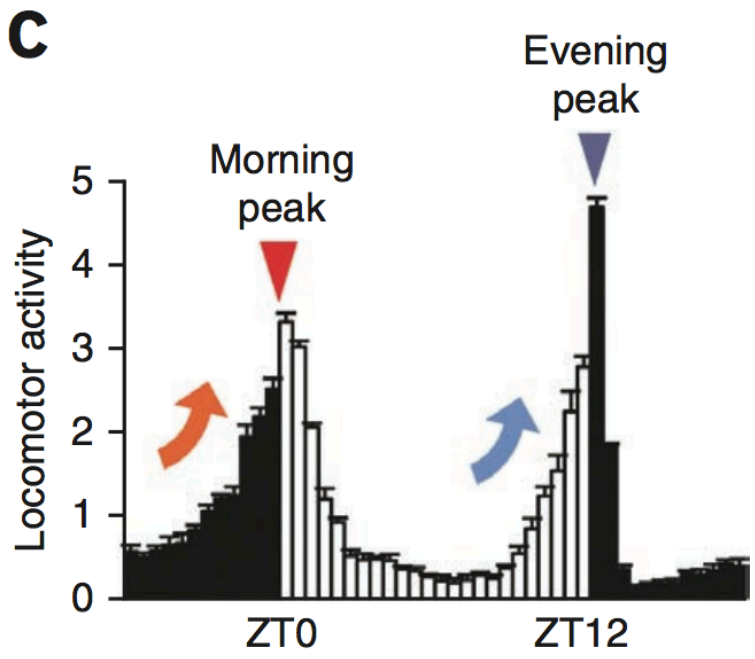

Figure I-3. Circadian behavior in *Drosophila* [10]

Drosophila locomotor activity displays a series of pattern with 24-hour periodicity under 12h light: 12h dark conditions. Zeitgeber time 0 (ZT0); time of lights on, ZT12; the time of lights off

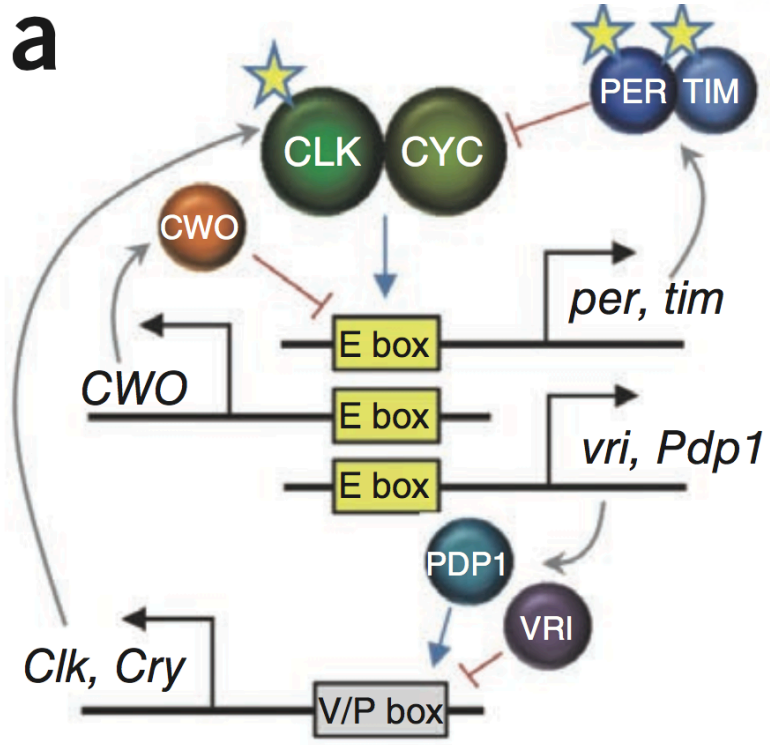

Figure I-4. Transcriptional feedback loops in *Drosophila* [10]

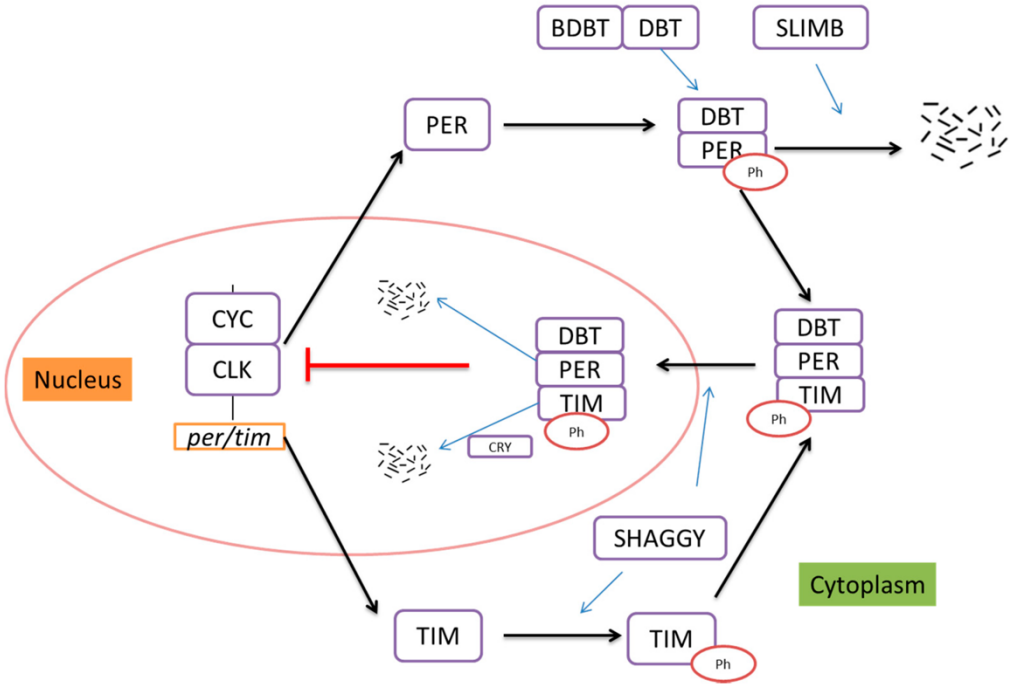

Figure I-5. Model of circadian clock in *Drosophila* [13]

I-3. Post-transcriptional regulation by ATAXIN-2 (ATX2) in circadian clock

In addition to transcriptional controls, post-transcriptional regulation is emerging as key modulators in molecular oscillation. Recently, the roles of RBPs in clock gene expression have been emphasized in regard to translational regulation and the RNA fate determination (**Figure I-6**) [10, 14]. In *Drosophila,* twenty-four (*tyf*) post-transcriptionally activates a translation of PER with poly A binding protein (PABP) association [15]. Because TYF lacks RNA-binding domains, additional factors should have been revealed for the translational activation of PER. A RNA-binding protein, ATAXIN-2 (ATX2) was identified as a coactivator of the TYF-dependent PER translation (**Figure I-7)** [16, 17]. TYF and ATX2 depletion using transgenic flies exhibit damaged circadian behaviors with decreased PER expression in pacemaker neurons [10, 15, 16]. Also, PABP association with TYF depends on C-terminal PABP-binding motif (PAM2) of ATX2 [16].

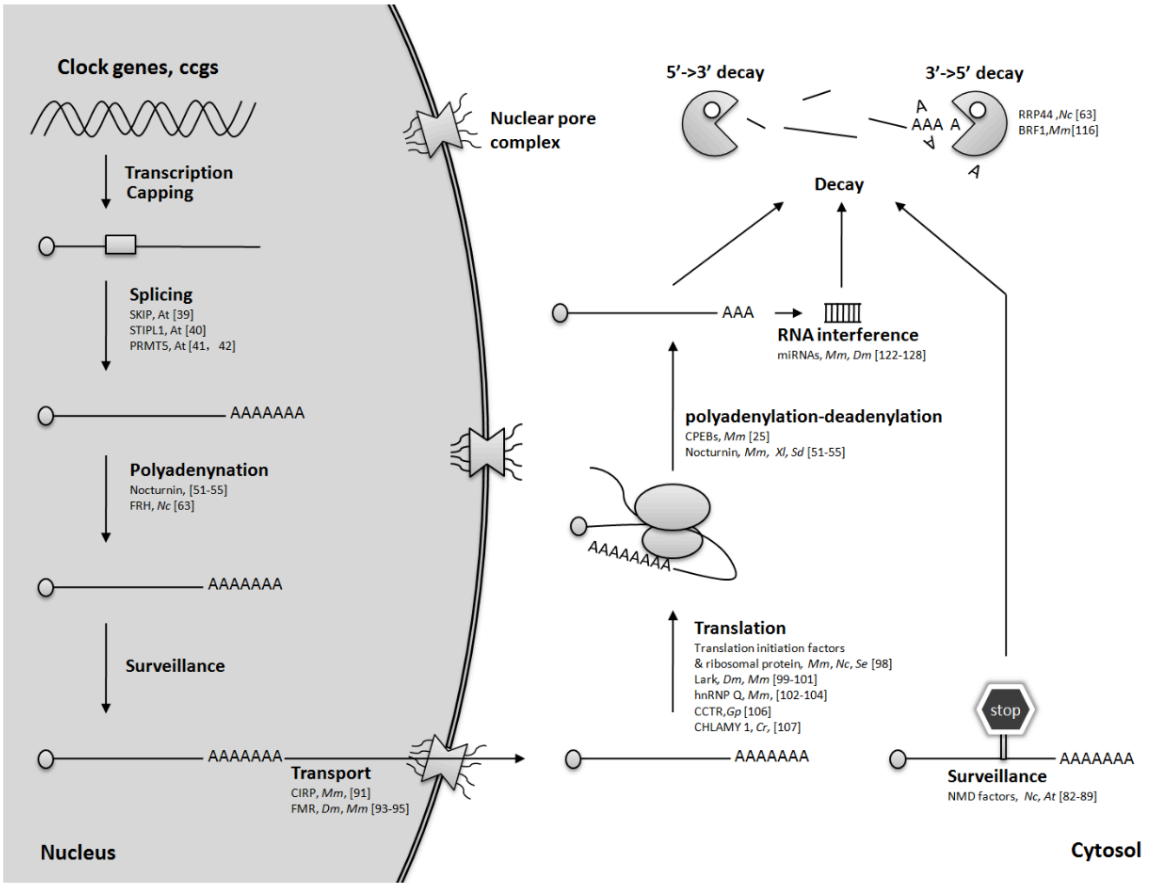

Figure I-6. Identified RNP complexes post-transcriptionally regulate clock gene expression [14]

Nc: *Neurospora crassa*; Mm: mammals; Dm: *Drosophila melanogaster*; At: *Arabidopsis thaliana*; Cr: *Chlamydomonas reinhardtii*; Gp: *Gonyaulax polyedra*; Se: *Synechococcus elongates*; Sd: *Suberites domuncul*a; Xl: *Xenopus laevis*

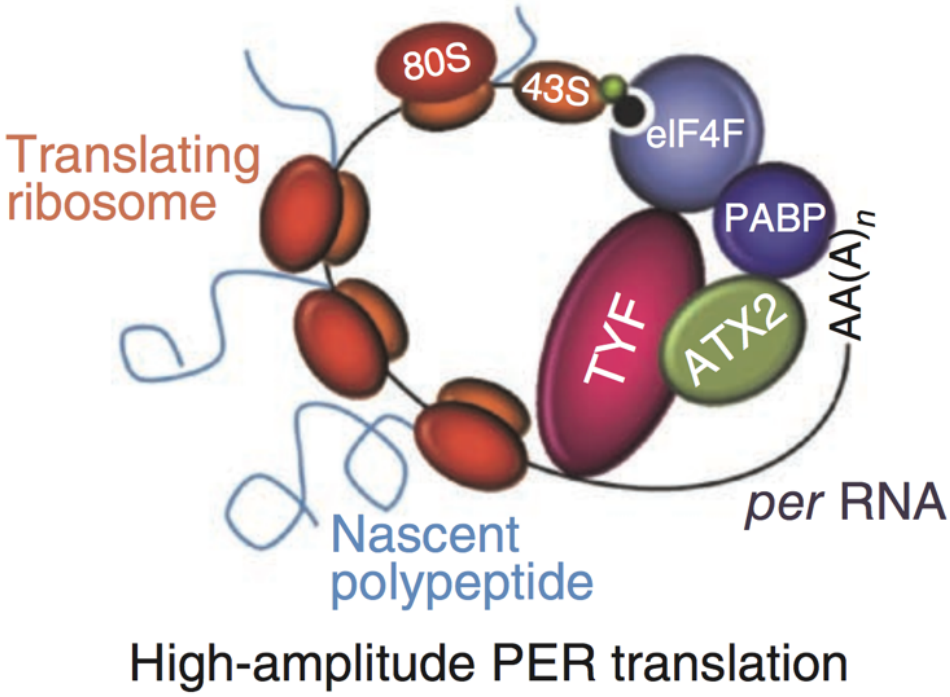

Figure I-7. TYF-ATX2 complex activates PER translation in circadian neurons [16]

I-4. ATAXIN-2 relevant diseases

RNA-binding proteins commonly cause degenerative diseases to promote the accumulation of nuclear or cytoplasmic RNA-protein (RNP) aggregates [18]. It leads to the imbalance in proteostasis. Mutational polyglutamine (polyQ) expansion in *human* ATAXIN-2 (ATXN2/ATX2) causes spinocerebellar ataxia type2 (SCA2) [19-21]. SCA2 is characterized by degeneration of Purkinje cells in the cerebellum, accompanying the progressive problems with movement and overall decline in intellectual function [22]. Intermediated-length polyQ tracts of ATX2 is a risk factor of amyotrophic lateral sclerosis (ALS), also known as Lou Gehrig's disease [23, 24]. The expanded polyQ tracts trigger its aggregation to produce toxic inclusion in cytoplasm. Actually, toxic ATX2 granules are detected in spinal cords of ALS patients (**Figure I-8**) [23].

The function of ATX2 is not completely characterized, but it has been suggested in regulating mRNA degradation, stability, and translation [25]. PAM2 domain of ATX2 modulates TDP-43 toxicity in ALS disease model [24]. Both polyQ and PAM2 also contribute to mRNA

stability and protein expression by direct binding to 3' untranslated region (3' UTR) of RNA [26]. Hereby, it implies the associating factors with ATX2 and translational functions of ATX2 might be crucial to generate ATX2-relevant diseases and discover therapeutic targets. Taken together, ATX2 is ultimately identified as a post-transcriptional regulator, but it remains elusive which specific factors assist ATX2-dependent translational modulations and how ATX2 controls gene expressions.

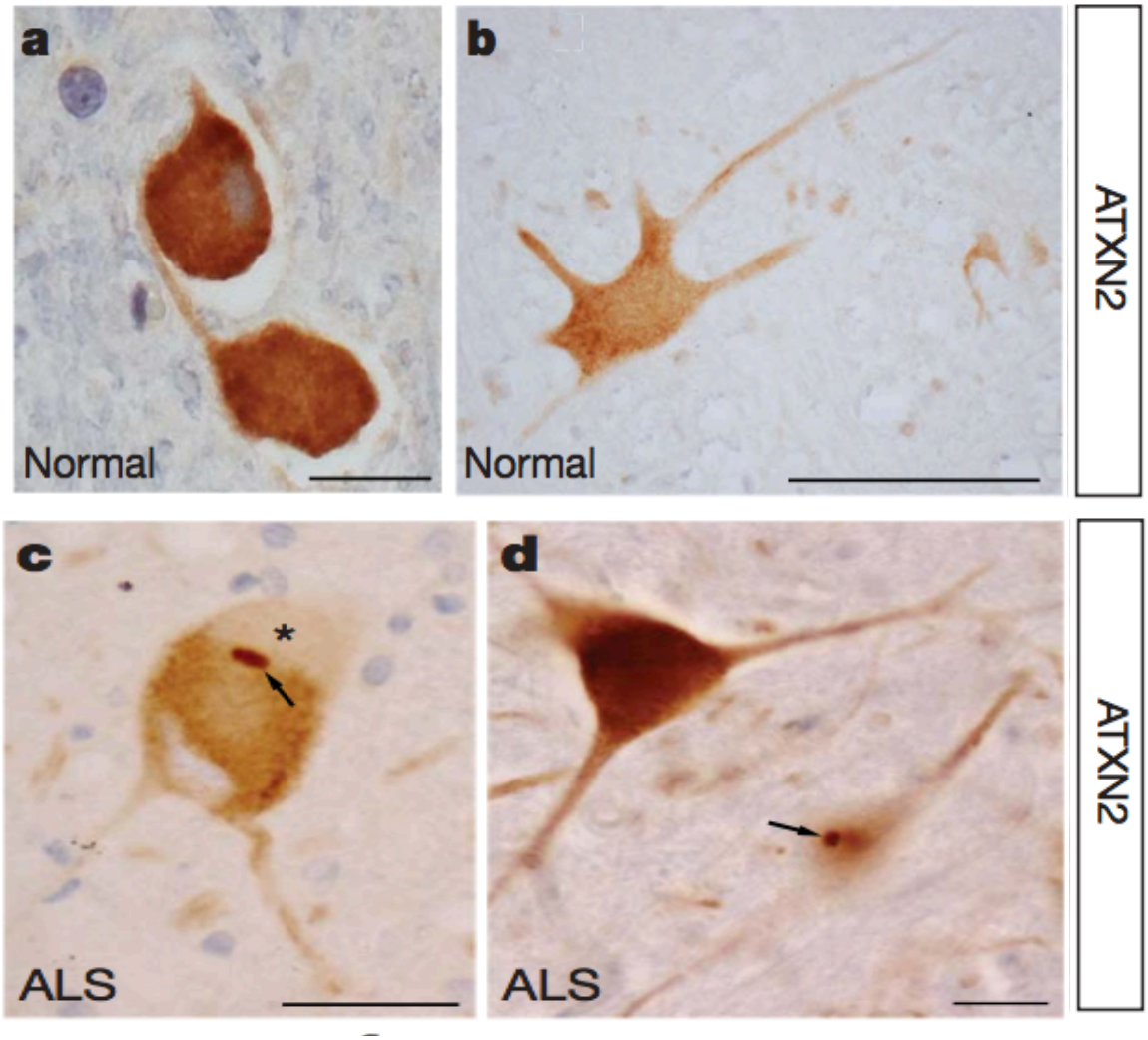

Figure I-8. toxic ATX2 granules in ALS patients [23]
ATXN2/ATX2 immunostaining in spinal cords of (a,b) normal person or (c,d) ALS patients . Arrows indicate toxic ATX2 granules.

II. Materials & Methods

Fly stocks

RNAi stocks (*Atx2* RNAi (v108843), *Lsm12* RNAi (v101762, T34666), *me31B* RNAi (T28566, T38923, 4916R-2)) were obtained from Bloomington *Drosophila* stock center, NIG-Fly stock center, and Vienna *Drosophila* RNAi center. *Pdf*-Gal4, *tim*-Gal4, *cry*-Gal4, Mz520-Gal4, UAS-TYFΔC5-3F, UAS-dicer2 transgenic lines were described previously [16]. Files were raised at 25°C on cornmeal/agar medium.

Measurement of circadian behaviors

Individual files were tested in single glass tube with 5% sucrose and 2% agar during 5 days in 12 hr light: 12 hr dark (LD) cycles and 7 days in constant darkness (DD). Flies were entrained in the LD cycles (light on, 8am; light off, 8pm) at 25°C. Circadian behaviors were determined by only internal clock in free running conditions (DD). Locomotor activities of individual flies were recorded at intervals of 1 min by the *Drosophila* Activity Monitor (DAM) system (TriKinetics). To obtain period and rhythmicity of each genotypes, time-based activity patterns for each 30 min interval from the beginning of DD cycles were analyzed using the ClockLab analysis software (Actimetrics).

Plasmids

S2 expression vectors for EGFP-Me31B, FLUC-boxB, FLUC-boxB-HhR, FLUC-boxB-HSL, FLUC-boxB-polyA-HhR, and FLUC-polyA-boxB-HhR were donated from E.Izaurralde [27, 28]. Also, ATX2-3F, ATX2-N-3F, ATX2ΔPAM2-3F, TYF-C5-3F, TYFΔC5-3F, MS2-V5, TYF-MS2-V5, and eIF4E-V5 were previously described [15, 16]. From the donated plasmids, I newly designed boxB-FLUC, boxB-FLUC-HhR, boxB-FLUC-HSL, 5' GTR-boxB-FLUC, 5' UTR-boxB-FLUC by inserting boxB and 3' modifications into pAC5.1-FLUC vector or 5' GTR-FLUC vector. 5' GTR was amplified from *per* 5' genomic UTR in fly heads. IRES reporters were originated from 5' IRES cDNA (CrPV derived IRES-RLUC, a gift from J.Imler [29]) with GFP sequence for first cistron. 3' modifications with boxB sites were inserted into GFP-IRES-RLUC (GFP-5'IRES). λN-fusion proteins were cloned from wild type or deletion mutants of ATX2, TYF (previously described [15, 16]), ME31B (EGFP-ME31B) by in-frame migration into pAC5.1B-λN-HA (a gift from E.Izaurralde). Additional ATX2 deletions (Δ855-890, Δ891-966, Δ855-966) were PCR-amplified by specific primers from ATX2 cDNA. NOT1-SD encoded amino acids of 909-1560 was PCR-amplified from NOT1 cDNA and inserted λN-HA vectors to express λN-HA-NOT1-SD.

Drosophila S2 cells and transfection

Drosophila Schneider 2 (S2) cells were cultured in Shields and Sang M3 insect medium (Sigma-Aldrich) supplemented with 10% fetal bovine serum and 1% penicillin-streptomycin (Thermo Fisher Scientific) at 25°C. For transient transfection, S2 cells were diluted at 1:2.6 from cell harvest and transfected with plasmid DNAs (400ng/1 well of 6-well plates) by Effectene Transfection Reagent (QIAGEN). After 48 hours from the transfection, S2 cells were prepared for next experiment.

RNAi-mediated depletion

For generating dsRNA, I designed specific primers containing T7 promoter in the both ends with desired DNA. A target was PCR-amplified by the primers with T7 promoter sequences which could initiate transcription. dsRNA was synthesized by T7-derived *in vitro* transcription using MEGAscript T7 kit (Thermo Fisher Scientific) and purified with DNase treatment, phenol-chloroform extraction, and ethanol precipitation. For the depletion in S2 cells, cells were handled with 1:2.6 dilution from growing cells. The 16 ug of dsRNA was treated on 6-well plates for immunoprecipitation and 8 ug was used on 12-well plates for luciferase assay. They were incubated for 4-5 days including a transfected period.

Luciferase assay

S2 cells were transfected with FLUC (10 ng), RLUC (10 ng), and expression vectors (180 ng) on 12-well plates. λN-fusion proteins or MS2-fusion proteins were used for following indication: 3' tethering assay including cap or IRES-dependent reporters, 15 ng; 5' tethering assay, 45 ng; the remainder (MS2 tethering assay, NOT1-dependent assay, 5' UTR-tethering assay), 180 ng. After 48 hours, cells were lysed by treatment of passive lysis buffer from Promega. Luciferase activity was measured using dual luciferase reporter assay kit (Promega).

Immunoprecipitation (IP) & Western blot

S2 cells were lysed with T300 buffer (25 mM Tris-Cl, pH 7.5, 300 mM NaCl, 10% glycerol, 25 mM EDTA, 1 mM dithiothreitol, 0.5% Nonidet P-40, and 1 mM phenyl-methylsulfonyl fluoride) at 4°C for 15 min with gentle rotation. By additional buffer without NaCl (T0 buffer) into cell lysates, the molar concentration of NaCl was adjusted to 150 mM. Soluble fractions of the lysates were obtained by centrifugation for 15 min at 13000 rpm. 30 ul of Input was prepared from the soluble extracts, and the rest was immunoprecipitated by indicated antibodies for 1.5 hr-2 hr at 4°C with gentle rotation including incubation time with specific beads. The beads were washed four times with T150 buffer (25 mM Tris-Cl, pH 7.5, 150 mM NaCl, 10% glycerol, 1 mM EDTA, 1 mM dithiothreitol, 0.5% Nonidet P-40, and 1 mM phenyl-methylsulfonyl fluoride). Prepared input and IP fractions were resolved by SDS-PAGE, usually 6% and 9.5%, and transferred to Protran nitrocellulose membranes (GE Healthcare). Indicated primary antibodies were used for detection of target protein. Horseradish

peroxidase-conjugated secondary antibodies (Jackson Immuno Research Laboratories) and Clarity Western ECL blotting substrate (Bio-Rad) were used. Finally, the protein levels in transferred blots were visible using ImageQuant LAS 4000 (GE Healthcare).

RNA preparation & realtime RT-PCR

Total RNAs were purified using Trizol reagent (Thermo Fisher Scientific) and treated to DNase (Promega) for digestion of remaining DNAs. The RNAs were isolated by phenol-chloroform extraction and ethanol precipitation. Then, they were reverse-transcribed into cDNAs by M-MLV reverse transcriptase (Promega) with random hexamers. Each target cDNAs was quantitatively analyzed by SYBR Green-based Prime Q-Mastermix (GeNet Bio) with indicated primers using LightCycler 480 realtime PCR system (Roche).

Gal4 & UAS system

Gal4-UAS system derived from yeast is well-established in *drosophila* to facilitate efficient regulations of targeted gene in a tissue- or cell-specific manner (**Figure II-1**) [30]. *Gal4* gene encodes the yeast transcription activator protein, GAL4, and it is expressed by such promoters targeting a specific tissue or cell type. UAS (upstream activation sequence) is a binding site of the GAL4 protein located in upstream of interest gene (gene X). The GAL4-UAS interaction promotes an expression of gene X in GAL4-expressing tissue.

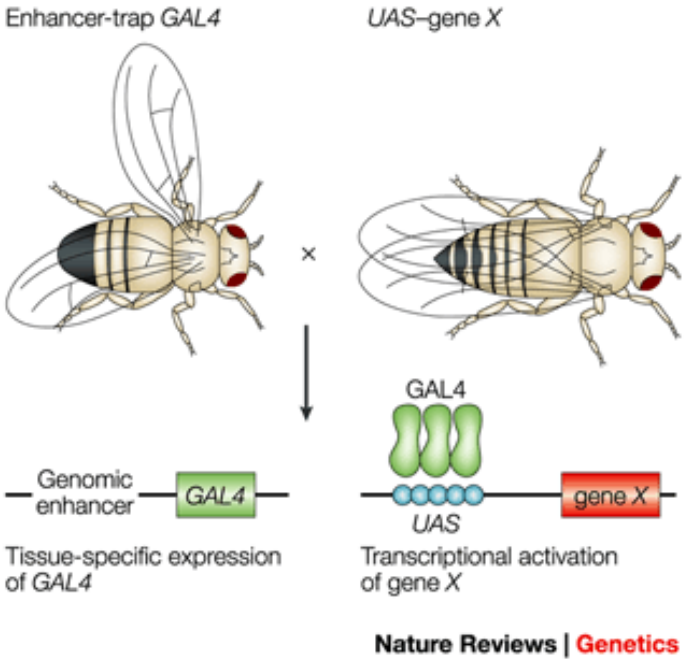

Figure II-1. GAL4-UAS system in *Drosophila* [30]

RNA-tethering system

RNA-protein interactions is artificially mimicked by the RNA-tethering system that is useful to study a translational regulation of RBPs on its target RNA. An interest protein (X) fused with tether protein is associated into tether binding site of reporter RNA and it would affect mRNA translation or stability (**Figure II-2)** [31]. The tethering system is based on bacteriophage proteins, MS2 coat protein or λN peptide. MS2 coat protein bind to a 21 nucleotide of RNA stem-loop with high specificity and selectivity allowing a high dosage of tethered proteins. Also, it acts on the target sequence as dimer. λN peptide is RNA binding motif interacting with 19 nucleotide of RNA hairpin in boxB that is early phage operons. Unlike the MS2 coat, it interacts with the tethering site (boxB) as monomer supporting 1:1 protein-RNA association. It minimizes potential interference with the fusion protein's function [31-33].

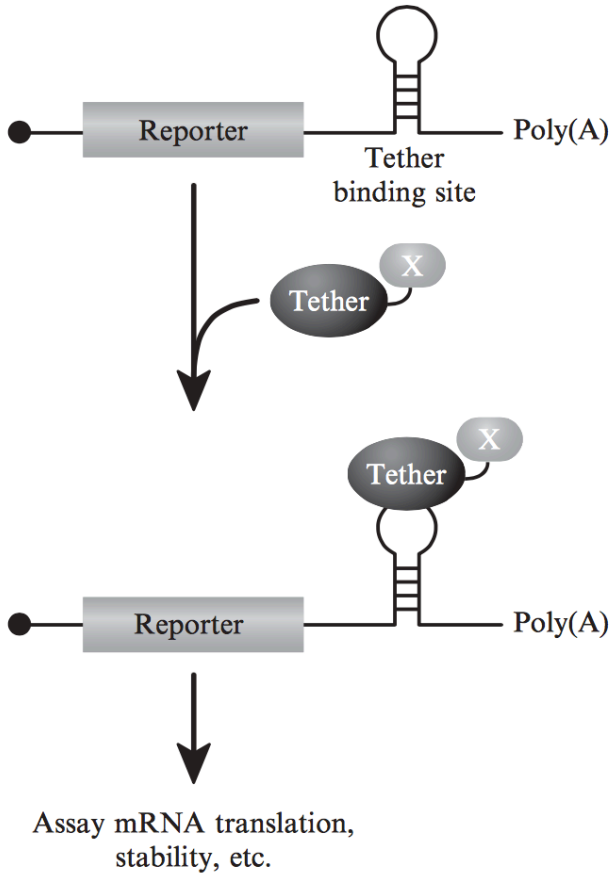

Figure II-2. RNA-tethering system [31]

III. Results

Part 1. Post-transcriptional regulation by ATX2 in *Drosophila*

III-1-1. Genetic screens demonstrate two different circadian behaviors with *Lsm12* or *me31B* depletion in clock neurons

In *Drosophila,* twenty-four (*tyf*) post-transcriptionally regulates circadian clocks to activate a translation of PER with PABP association [15]. In the following research, a RNA-binding protein, ATAXIN-2 (ATX2) was identified as a coactivator of the TYF-dependent PER translation [16, 17]. These ATX2-TYF complex function as activator in *Drosophila*, but there was potential for the presence of additional factors in the complex. To discover new novel factors for ATX2-dependent translation, I employed genetic screening in circadian behaviors with *drosophila* model on the basis of previous study. With Gal4-UAS system, candidate genes were depleted by expressing RNA interference (RNAi) in clock neurons. I used *tim*-Gal4 and *Pdf*-Gal4 for targeting all or partial clock neurons with UAS-DICER2 for efficient RNAi expression (each called TD2, PD2). As a result, I found two distinct phenotypes in depletion of *CG1573*, a *Drosophila* homolog of *Lsm12*, and *me31B*, a *Drosophila* homolog of the ATP-dependent RNA helicase *DDX6/Rck/p54*. Two independent *Lsm12* RNAi lines show long period locomotor activity with normal rhythmicity compared to controls (**Figure III-1A, B**). By contrast, three *me31B* RNAi lines exhibit normal periodicity with poor rhythm (**Figure III-1A, C**). These data suggest LSM12 and ME31B contributes to circadian clocks via different regulatory mechanisms.

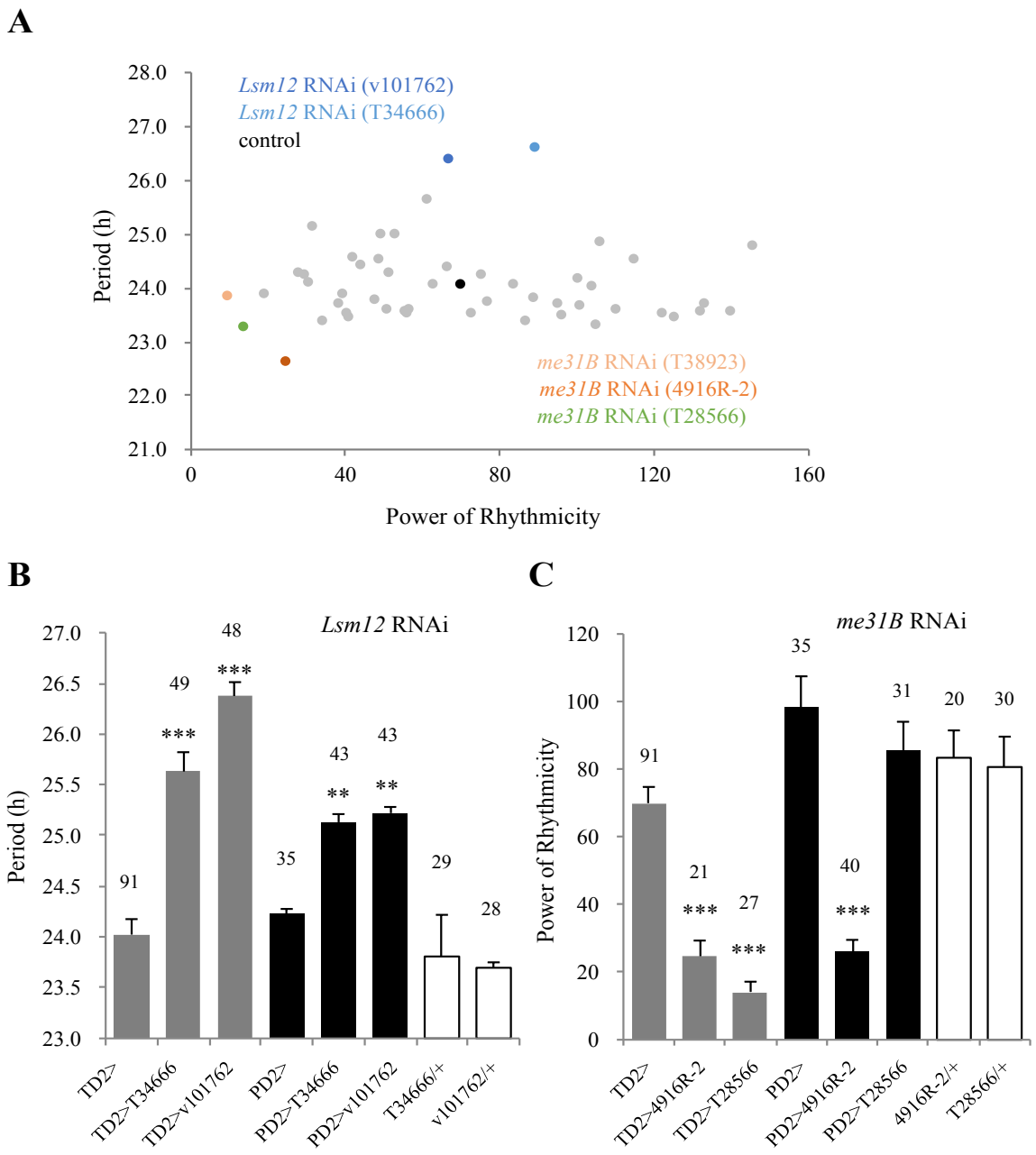

Figure III-1. *Lsm12* and *me31B* depletion causes disturbed circadian behavior in *Drosophila*

(A)Genetic screening for candidate genes to interact with ATX2 in clock neurons. Each RNAi transgene is expressed by tim-Gal4 with UAS-dicer2 (TD2) for efficient RNAi application. Circadian periods were determined by chi-square periodograms in dark:dark cycles and power of rhythmicity calculated by power(P, rhythmic strength) minus significance(S) values. n=12~105 (B)*Lsm12* depleted flies show lengthened circadian period in TIM and PDF(PD2)-expressing neurons. (C)*Me31B* knockdown in clock-dependent neurons results in poor rhythmicity. (B, C)The number of analyzed flies are indicated above each graphs. Data represent mean and SEM. $^{**}p < 0.01$, $^{***}p < 0.001$ compared to each heterozygous controls by one-way ANOVA, Tukey's post hoc test.

III-1-2. LSM12 and ME31B genetically interacts with ATX2 in *Drosophila*

In the genetic screening, each depletion of LSM12 and ME31B affects circadian period and rhythmicity in *Drosophila.* I wondered whether the phenotypes from two factors are dependent on ATX2-related physiology or not. To address these question, I first checked genetic interaction of *Lsm12* and *me31B* with ATX2-TYF complex. C5 domain of TYF is crucial for its translational activation [16]. *Lsm12* depletion exaggerates lengthened period by expressing TYF dominant-negative (TYFΔC5) transgene in pace-maker neurons, but *me31B* does not affect to the phenotype (**Figure III-2A**). Also, knockdown of *me31B* aggravates circadian rhythmicity with the expression of *Atx2* RNAi in cry-dependent clock neurons (**Figure III-2B**).

III-1-3. ATX2 associates with LSM12 and ME31B in *Drosophila* S2 cell

In addition to genetic interaction of *Lsm12* and *me31B* with *Atx2*, I examined these two factors could associate with ATX2 complex by direct binding. I used immunoprecipitation (IP) with endogenous or tag-specific antibodies after transfection in S2 cells (*Drosophila* embryo cells). Actually, LSM12 interacts with ATX2-TYF complex in an RNA-independent manner (**Figure III-3A**). ME31B is also revealed as a component of the complex (**Figure III-3B**). Taken together, LSM12 and ME31B are identified as new factors for ATX2 macromolecular complex in *Drosophila*.

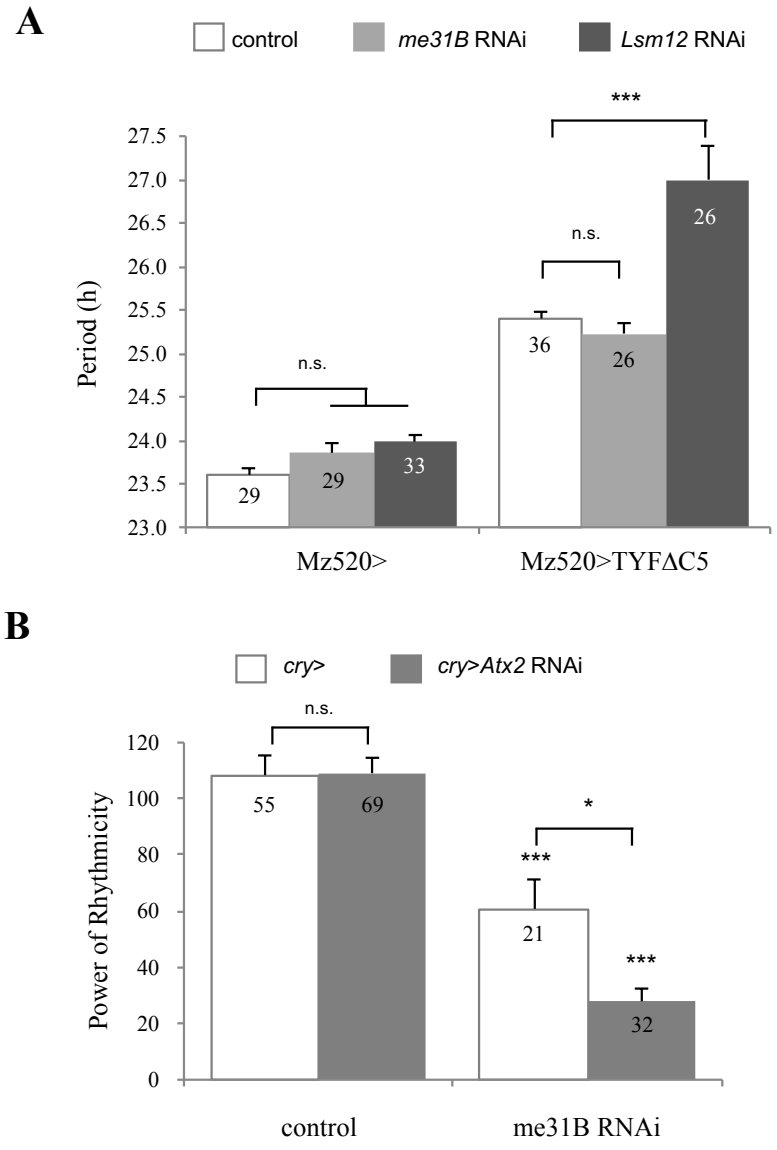

Figure III-2. Genetic interaction of *Atx2* with *Lsm12* and *me31B* in circadian-dependent manner (A)*Lsm12* depletion in PDF neurons (Mz520-Gal4) exaggerates lengthened period by TYF dominant-negative mutants (TYFΔC5). The *me31B* doesn't affect TYF-dependent circadian phenotypes. (B)*Atx2* RNAi expression in cry-relevant clock neurons synergistically reduces power of rhythmicity with *me31B* depletion. The number of analyzed flies is indicated in each graphs. Data represent mean and SEM. n.s., not significant, $^{*}p < 0.05$, $^{***}p < 0.001$ compared to control for the *me31B* RNAi by one-way ANOVA, Tukey's post hoc test.

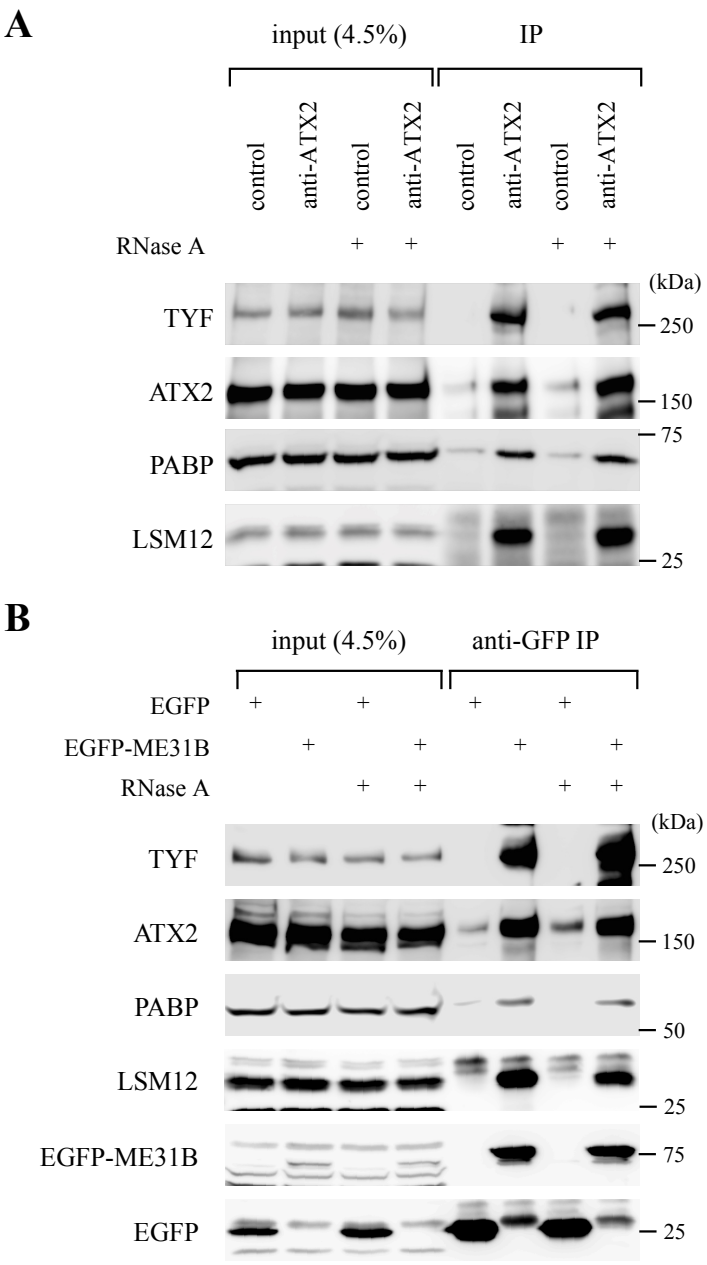

Figure III-3. ATX2 interacts with LSM12 and ME31B in RNA-independent manner in *Drosophila* S2 cell

(A)Cell extracts treated with or without 0.5 mg/ml RNase A were immunoprecipitated by pre-immune serum (control) or anti-ATX2 antibodies. Purified IP complexes were analyzed by western blotting and detected with specific antibodies (left). (B)Where indicated, S2 cells were transfected with EGFP or EGFP-ME31B expression vectors. After 48 hours from the transfection, soluble extracts are prepared with or without 0.5 mg/ml RNase A treatment. The soluble extracts are immunoprecipitated by anti-GFP antibody. The IP complexes were also analyzed similarly as above.

III-1-4. LSM12 acts as an adaptor for ATX2-TYF interaction

To elucidate LSM12 roles and features in ATX2-TYF complex, I compared physical interactions in the complex by immunoprecipitation (IP) with control or LSM12-depleted cell. ATX2 interacts with C5 domain in TYF for a translational activation and acts as co-activator [16]. LSM12 depletion causes disruption of ATX2-TYF(C5) interaction, while ATX2 associates with TYF-C5 in control (**Figure III-4**). Deletion of C5 domain (ΔC5) cannot interact with both ATX2 and LSM12. These data demonstrate LSM12 acts as an adaptor for ATX2-TYF interaction.

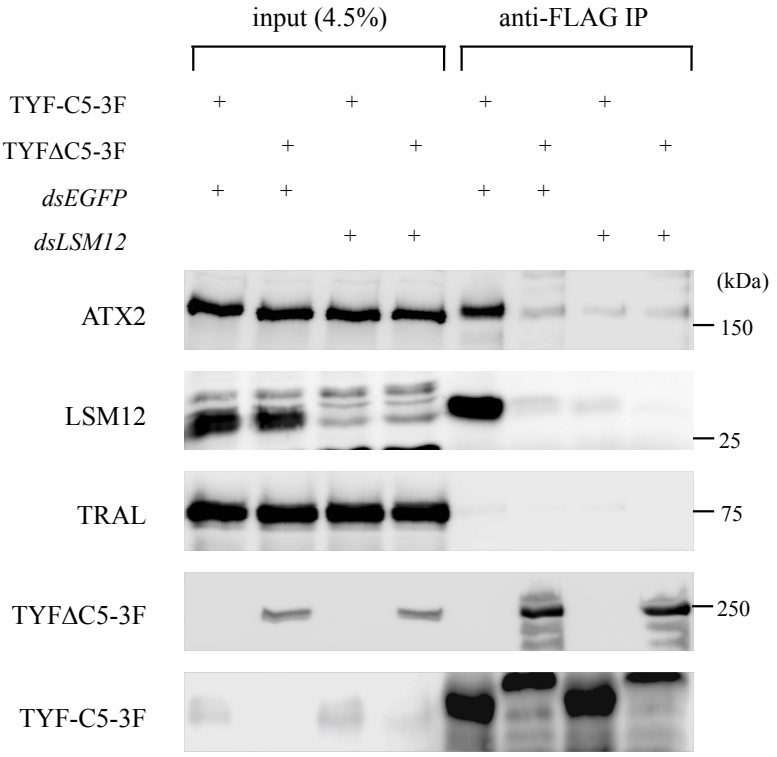

Figure III-4. LSM12 is necessary for ATX2-TYF interaction as an adaptor
ATX2 and LSM12 interacts with TYF-C5 (translational activation domain). LSM12 depletion blocks ATX2 association from TYF complex. For control or LSM12 knockdown, S2 cells are treated with *dsEGFP* or *dsLSM12*. After 3days, each depleted cells are transfected with flag-tagged TYF-C5 or TYFΔC5 expression vectors. Soluble extracts are prepared and immunoprecipitated by anti-FLAG antibody after 2days from the transfection. IP complexes were analyzed by western blotting and detected with specific antibodies (left).

III-1-5. LSM12 facilitates TYF-dependent translational activation through ATX2 interaction

The ATX2-TYF complex activate *period* expression in clock neurons [16]. According to previous data, I thought LSM12 might have a role in TYF-dependent translational activation. To address these questions, I employed RNA tethering assay with LSM12 depletion. Importantly, TYF-specific activation significantly decreases in LSM12 depletion (**Figure III-5A**). Reduction of LSM12 protein by *dsLSM12* treatment is verified by western blot (**Figure III-5B**). The translational efficiency is highly dependent on initiation steps through the association of cap-binding proteins for ribosome recruitment [34]. Thus, I did immunoprecipitation in S2 cells transfected with v5-tagged eIF4E by anti-v5 antibody. Direct cap-binding protein, eIF4E, assembles all ATX2, LSM12, and TYF into translational initiation complex (**Figure III-6**). Additionally, I did cap binding assay with each knockdown of the components. As a result, ATX2 depletion induces the dissociation of LSM12 and TYF from 5' cap (**Figure III-7**). These data suggest ATX2 triggers 5' cap association of LSM12 and TYF for the translational activation.

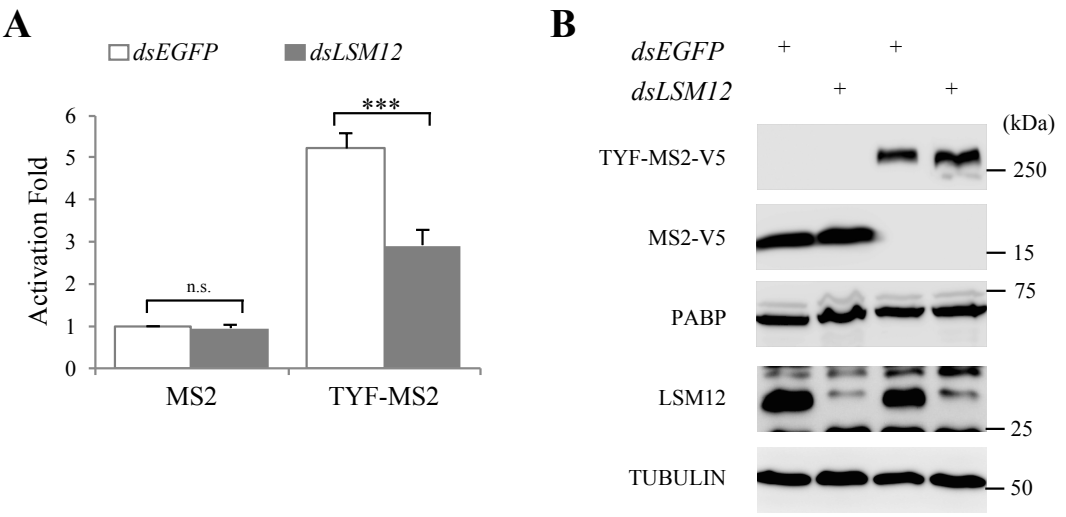

Figure III-5. LSM12 mediates TYF-dependent activation of gene expression

(A)LSM12 depletion blocks TYF-specific activation in S2 cell. Soluble extracts are prepared for luciferase assay and co-transfected with firefly luciferase (FLUC) containing MS2 binding sites, *Renilla* luciferase (RLUC) and MS2 fusion proteins (MS2 or MS2-TYF) in EGFP or LSM12-depleted cells. FLUC/RLUC compared with MS2-tethering value in EGFP knockdown cell and this indicates activation fold. Data represent mean and SEM of 5 independent experiments. n.s., not significant, $^{***}p < 0.001$ analyzed by one-way ANOVA, Tukey's post hoc test. (B)LSM12 depletion is confirmed by western blotting and detected with specific antibodies (left).

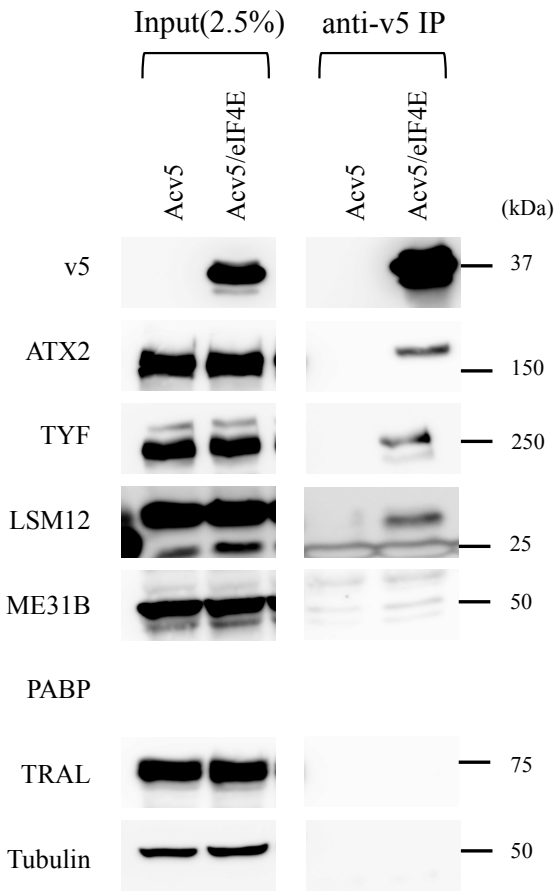

Figure III-6. Activator complex, ATX2-LSM12-TYF, associates with a cap binding protein, eIF4E ATX2-LSM12-TYF complex interacts with eIF4E. S2 cell is transfected with v5 or v5-tagged eIF4E and immunoprecipitated by anti-v5 antibody. Purified IP complexes were analyzed by western blotting and detected with specific antibodies (left).

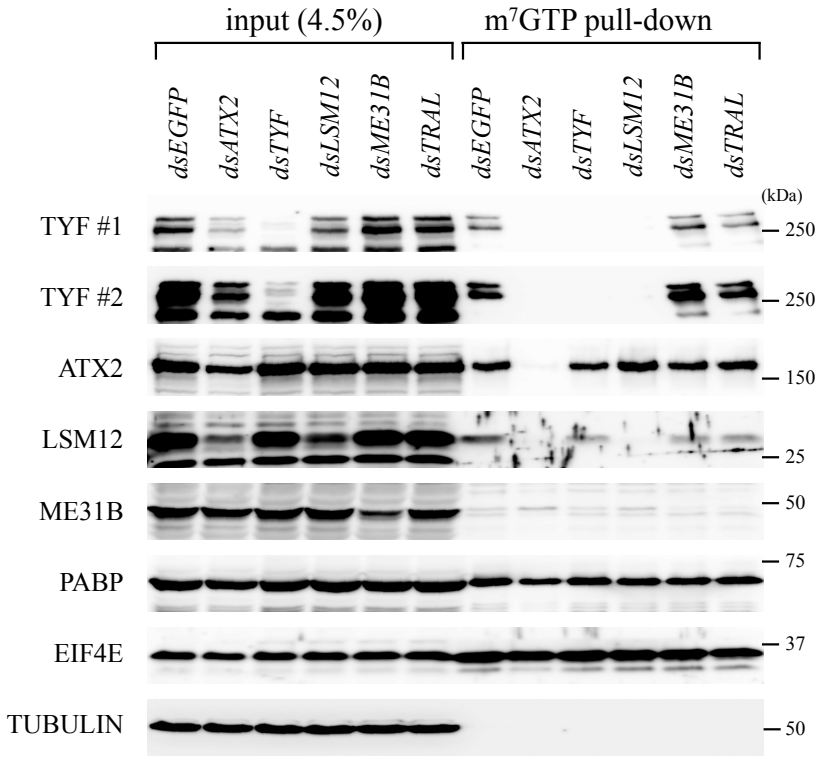

Figure III-7. ATX2 facilitates the association of LSM12 and TYF into 5' cap-relevant translation initiation complex

ATX2 depletion inhibits 5' cap association of LSM12 and TYF and LSM12 knockdown blocks only TYF assembly to the 5' cap. EIF4E is positive control and TUBULIN is negative control for the experiment. Each depleted cells as indicated above are immunopricipitated by m^7GTP affinity beads to isolate cap-binding complexes. Purified IP complexes were analyzed by western blotting and detected with specific antibodies (left).

III-1-6. ATX2-ME31B interacts with NOT1 accompanied by NOT1-dependent gene silencing

Unlike ATX2-LSM12-TYF complex, ME31B is not associated with 5' cap in the assay (**Figure III-6, Figure III-7**). It indicates ME31B has an independent mechanism with ATX2 interaction. ME31B/DDX6 has been implicated as a translational repressor and decapping activator participating in microRNA (miRNA) mediated gene silencing through CCR4-NOT deadenylase complex by direct interaction with NOT1 [35-38]. Accordingly, ATX2-ME31B complex might follow NOT1-dependent silencing pathway. To prove that, I first immunoprecipitated flag tagged N-terminal ATX2 in ME31B or LSM12 depletion (**Figure III-8**). N-terminal ATX2 is sufficient for interaction with LSM12 and ME31B (data not shown). The data demonstrate NOT1 also interacts with N-terminal ATX2. Importantly, NOT1-ATX2 interaction is disrupted by ME31B depletion, while ATX2-LSM12-TYF complex is not influenced. In addition, LSM12 depletion cannot affect ME31B and NOT1 association to ATX2. These results suggest ATX2-ME31B-NOT1 complex is independent on the translation activation complex, ATX2-LSM12-TYF.

To identify a function of ATX2-ME31B-NOT1 complex, I employed RNA-tethering assay with NOT1 silencing domain (SD) composed of the amino acids from 909 to 1,560. This domain corresponds with a homologous region of human NOT1 involved in DDX6 binding and DDX6-dependent gene silencing [35-38]. By NOT1 SD tethering, FLUC expression of all reporters (FLUC-boxB, FLUC-boxB-HhR, FLUC-boxB-HSL, [27, 39, 40]) is repressed with 2.5 to 4 fold changes. ME31B depletion causes significant de-repression in FLUC-boxB-HSL reporter. Interestingly, ATX2 also assists Not1-mediated gene silencing consistent with ME31B (**Figure III-9A**). The FLUC-boxB-HSL reporter is deficient in poly A tail, but it is able to circularize itself (**Figure III-9B**). It supports ATX2-ME31B-NOT1 complex might specifically target circularized and poly A-deficient transcripts. Taken together, ATX2 associates with ME31B-NOT1 and functions as a repressor in specific transcripts via NOT1-mediated silencing mechanism.

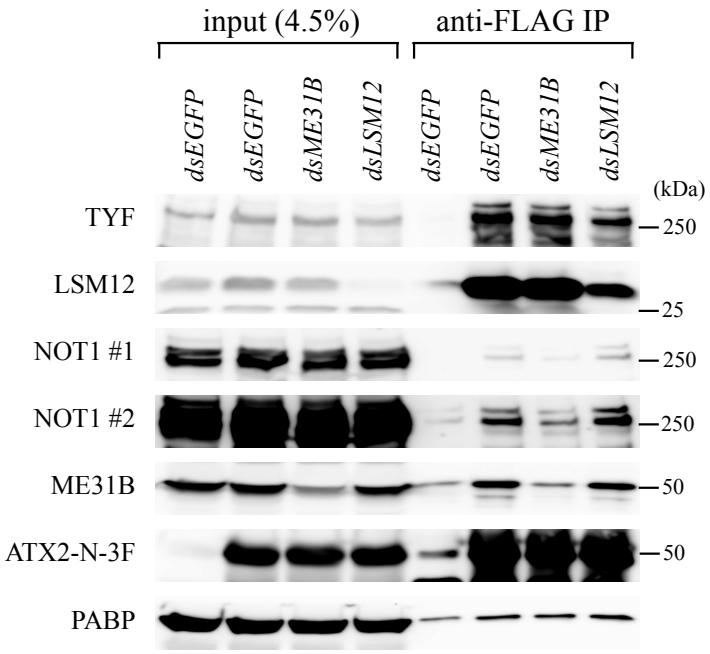

Figure III-8. ME31B mediates ATX2-NOT1 interaction in *Drosophila* S2 cell

ME31B depletion causes dissociation of NOT1 from ATX2 complex. After 3days from dsRNA treatment for knockdown of each component, S2 cells are transfected with flag-tagged N-terminal ATX2 and immnoprecipitated by anti-FLAG antibody. Purified IP complexes were analyzed by western blotting and detected with specific antibodies (left).

A

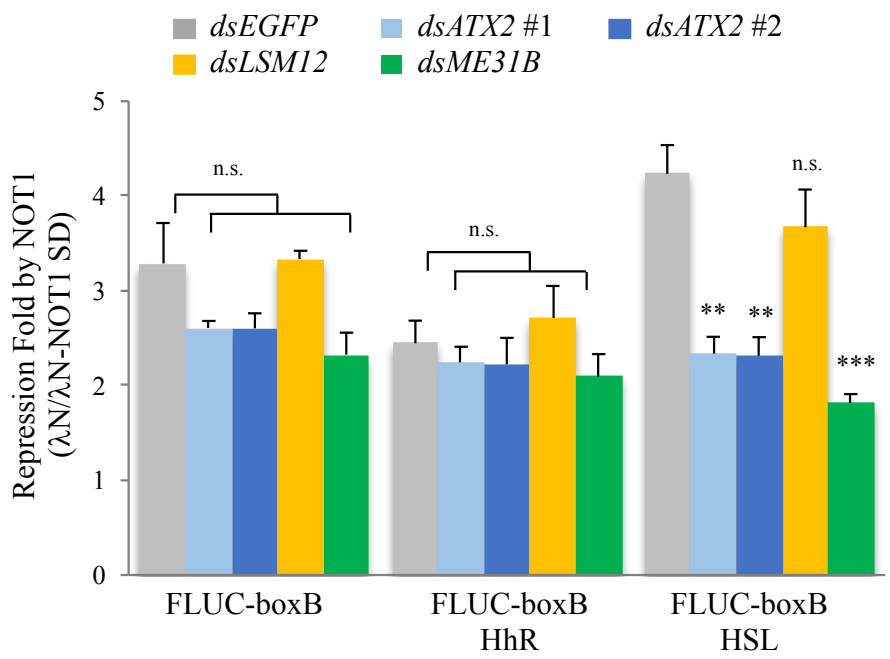

B

	Poly A tail	Circularization
FLUC-boxB	O	O
FLUC-boxB-HhR	X	X
FLUC-boxB-HSL	X	O

Figure III-9. ATX2 participates in NOT1-mediated gene silencing dependent on ME31B interaction (A)ATX2 and ME31B depleted cells show de-repression on FLUC-boxB-HSL in the NOT1-dependent context. S2 cells are co-transfected with 3' modified FLUC containing binding sites for λN fusion proteins (boxB), RLUC, and λN fusion proteins (λN or λN-NOT1 SD). After 48 hours from the transfection, soluble extracts are prepared and analyzed by dual luciferase assay. FLUC/RLUC compared with λN-tethering value in EGFP knockdown cell and this indicates repression fold. Data represent mean and SEM of 3 independent experiments. n.s., not significant, $^{**}p < 0.01$, $^{***}p < 0.001$ analyzed by one-way ANOVA, Tukey's post hoc test. (B)Summarized table for 3' modified tethering reporters in (A) experiment. FLUC-boxB includes poly A tail and it can be circularized. FLUC-boxB-HhR indicates 3' modified reporter of FLUC-boxB with hammerhead ribozyme (HhR). FLUC-boxB-HSL also represents a transformed FLUC-boxB reporter with histone stem-loop (HSL) at 3' end. The HhR and HSL sequences substitute Simian virus 40 (SV40) Poly A signal to exclude poly A tail. As indicated in the table, a HhR reporter cannot be circularized by the ribozyme and HSL-binding protein can associate with translation initiation factor to promote RNA circularization [27, 39, 40].

Part 2. Roles of ATX2 on mRNA translation in *Drosophila* S2 cell

III-2-1. ATX2 activates translation in 3' RNA tethering system

Although I obtained information about ATX2-associating factors on circadian clock, it remains elusive how ATX2-dependent gene expression is regulated. To investigate ATX2 roles in mRNA translation, I mimicked several mRNA features with artificial reporters that could be tethering target proteins (**Figure III-10A**). The reporters have five boxB sequences capable of interaction with λN-tagged protein following firefly luciferase (FLUC) [27, 39, 40]. For more diverse mRNA features, I used other tethering reporters with 3' modification in Simian virus 40 (SV40) Poly A signal which can terminate a transcription and add poly A tail to mRNA. According to the existence of poly A tail and possibility of RNA circularization, the reporters are classified (**Figure III-9B**). ATX2-tethering on 3' end of RNA promotes FLUC expression about 3 to 6 folds compared with controls in S2 cell (**Figure III-10B**). Especially, ATX2-specific activation reveals more remarkable effects in FLUC-boxB-HhR, while a change of mRNA levels by ATX2-tethering is similar in all reporters (**Figure III-10C**). It indicates there might be a translational activation mechanism depending on ATX2 rather than RNA stability in the FLUC-boxB-HhR reporter. Moreover, the roles of ATX2 in translation might be strengthened in non-polyadenylated (or short-poly A tailing) and non-circularized transcripts.

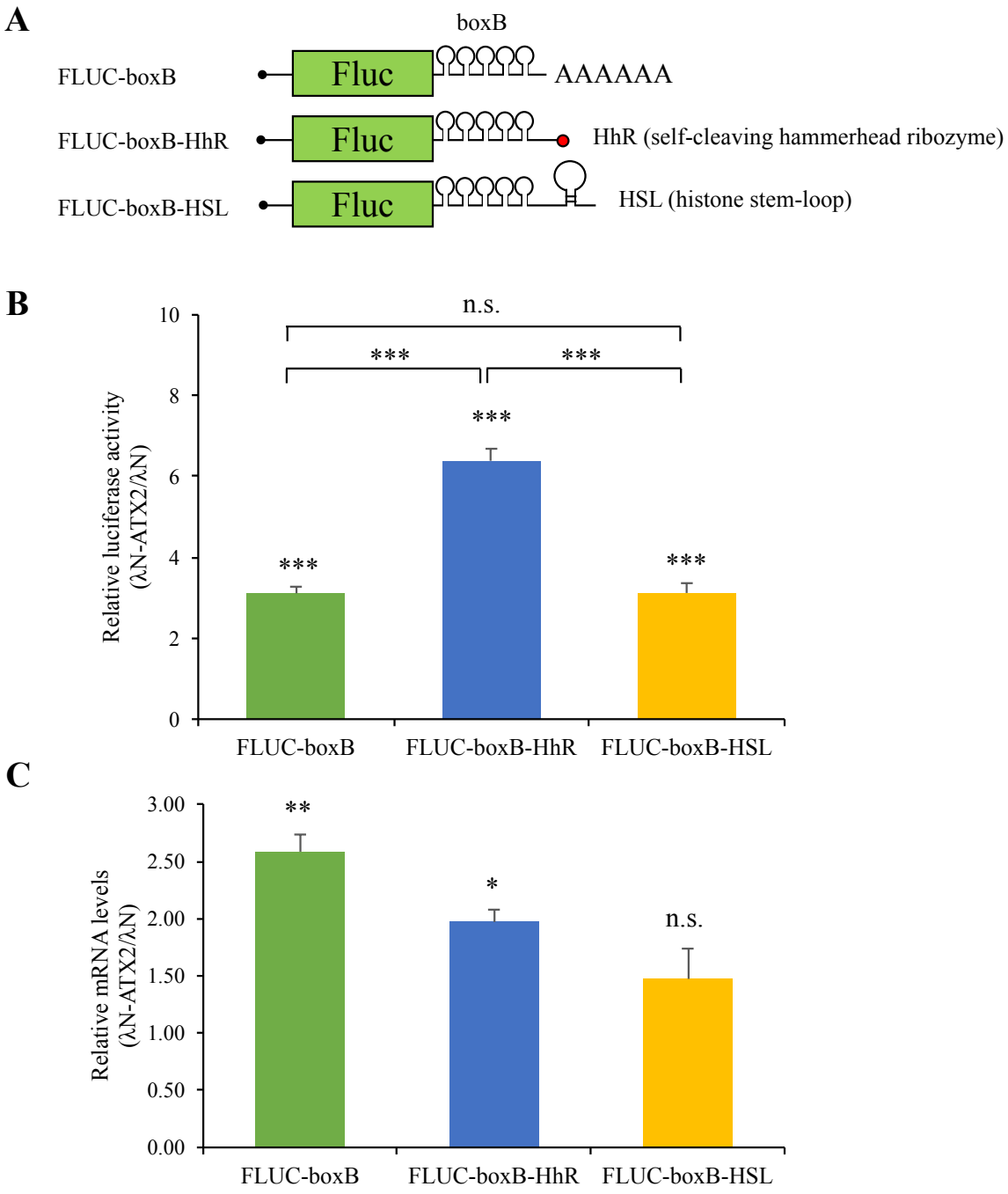

Figure III-10. ATX2 activates FLUC expression on 3' of transcripts

(A)Schematic diagram of 3' tethering reporters. FLUC-boxB, Firefly luciferase-5x boxB (λN binding site)-poly A tail; FLUC-boxB-HhR, Firefly luciferase-5x boxB-HhR (self-cleaving hammerhead ribozmyme) instead of poly A tail; FLUC-boxB-HSL, Firefly luciferase-5x boxB-HSL (histone stem-loop) instead of poly A tail (B)ATX2 on 3' RNA promotes its translation, especially in HhR-modified reporter. S2 cell is transfected with FLUC reporter as indicated, RLUC, and λN-tagged proteins (λN or λN-ATX2). After 48 hours from that, soluble extracts are prepared and monitored by dual luciferase assay. FLUC expression is normalized by RLUC in each samples. The relative levels are calculated by

normalizing each FLUC/RLUC to λN-tethering values (λN-ATX2/λN). Data represent mean and SEM of 6 independent experiments. (C)ATX2 stabilizes the transcripts, but the fold changes are relatively similar in all reporters. Total RNAs were prepared from transfected S2 cell with each FLUC reporter, RLUC, and λN-tagged proteins (λN or λN-ATX2). mRNA levels of FLUC is analyzed by realtime RT-PCR and normalized by RLUC in each samples. The relative levels are calculated as same way in above luciferase assay. Data represent mean and SEM of 3 independent experiments. n.s., not significant, $^{*}p < 0.05$, $^{**}p < 0.01$, $^{***}p < 0.001$ analyzed by one-way ANOVA, Tukey's post hoc test, compared to λN protein tethering on each indicated FLUC reporters.

III-2-2. Domain mapping for ATX2-specific activation validates an importance of ATX2-PABP interaction

To identify a domain for the translational activation, I used the RNA-tethering assay with ATX2 deletions (**Figure III-11A**). This mapping reveals poly(A)-binding protein (PABP)-interacting motif 2 (PAM2) is critical for the activation (**Figure III-11B**). PABP directly interacts with translation initiation factor, eIF4G, inducing mRNA circularization that stimulates ribosome recycling and enhances translation efficiency by promoting the recruitment of cap-binding proteins to 5' cap [6-9]. In addition to ΔPAM2 data, PABP knockdown by *dsPABP* treatment impedes ATX2-specific activation (**Figure III-12A**). In particular, FLUC-boxB-HhR shows significant deactivation by PABP depletion, suggesting RNA circularization by ATX2-PABP interaction leads to high efficient translation on poly A-deficient transcripts. The increased RNA stability by ATX2 possibly contributes to remaining activation despite PABP knockdown (**Figure III-10C, Figure III-12A**). PABP levels is actually reduced by the dsRNA treatment (**Figure III-12B**).

III-2-3. The poly A tail existence masks ATX2-specific activation on FLUC-boxB-HhR

For more insights about HhR reporter, I tested additional reporters including a HhR sequence with poly A tail (**Figure III-13A**). The poly A tail is located between FLUC and boxB sequences (FLUC-polyA-boxB-HhR) or between boxB and HhR sequences (FLUC-boxB-polyA-HhR). Both poly A tailed HhR reporters show decreased fold changes compared with poly A tail-deficient HhR reporter (Fluc-boxB-HhR) (**Figure III-13B**). Those reporters display similar levels to FLUC-boxB which has poly A tail with circularization. These data suggest the restoration of poly A tail in a HhR reporter partly mimics circularizing effect.

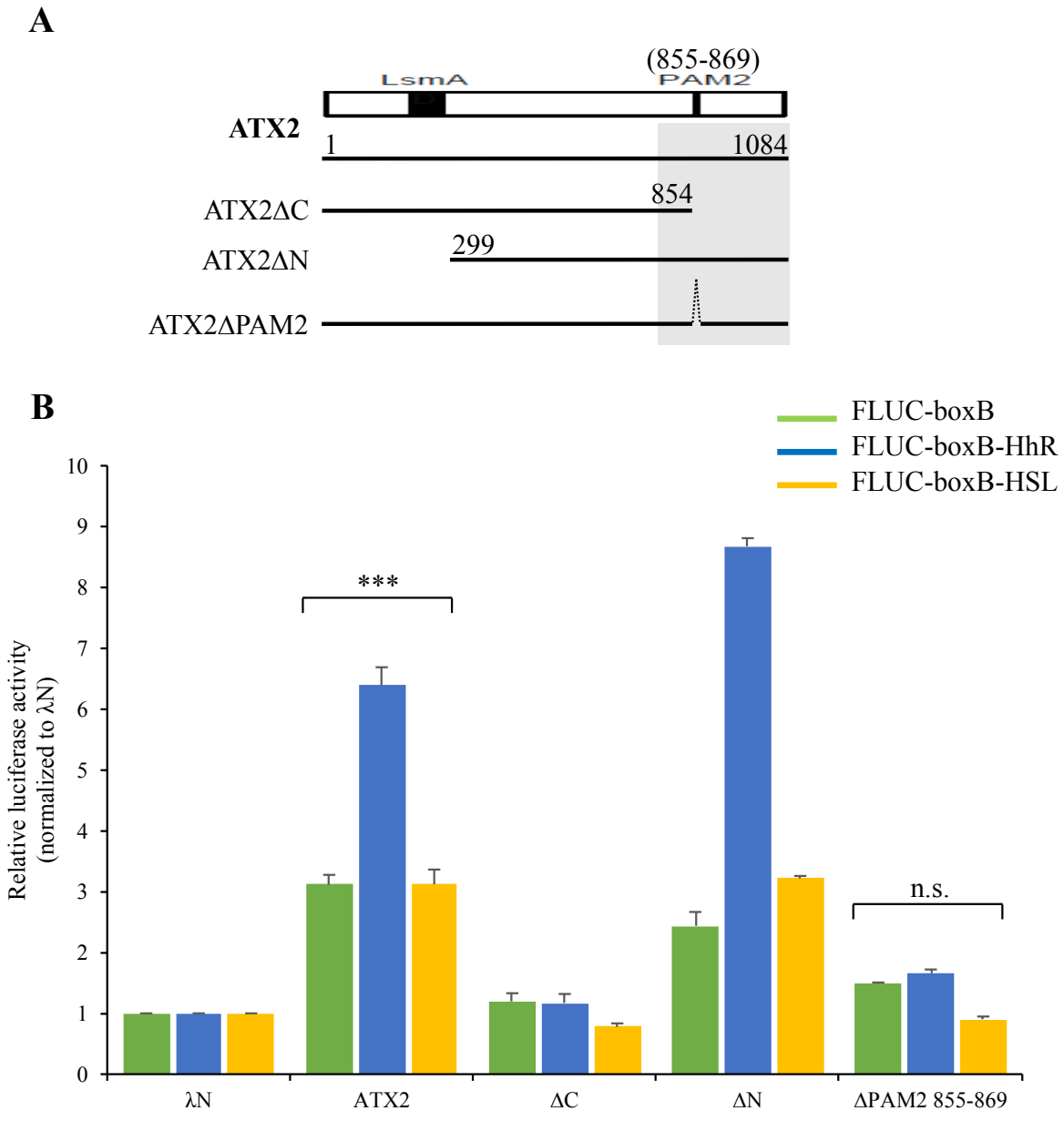

Figure III-11. PABP-interacting motif (PAM2) of ATX2 is crucial for the translational activation (A)ATX2 deletions for domain mapping of ATX2 activation. ATX2ΔPAM2; deletion of PAM2 domain(Δ855-869); Δ indicates deleted DNA constructs of each domain (N, C, PAM2). (B)ATX2ΔPAM2 disrupts ATX2-specific activation in the 3' tethering reporters. S2 cell is transfected with FLUC reporter as indicated, RLUC, and λN-tagged proteins (λN or λN-ATX2 deletions). After 48 hours from that, soluble extracts are prepared and monitored by dual luciferase assay. FLUC expression is normalized by RLUC in each samples. The relative levels are calculated by normalizing each FLUC/RLUC to λN-tethering values. Data represent mean and SEM of 4-6 independent experiments. n.s., not significant, $^{***}p < 0.001$ analyzed by one-way ANOVA, Tukey's post hoc test, compared to λN protein tethering on each indicated FLUC reporters.

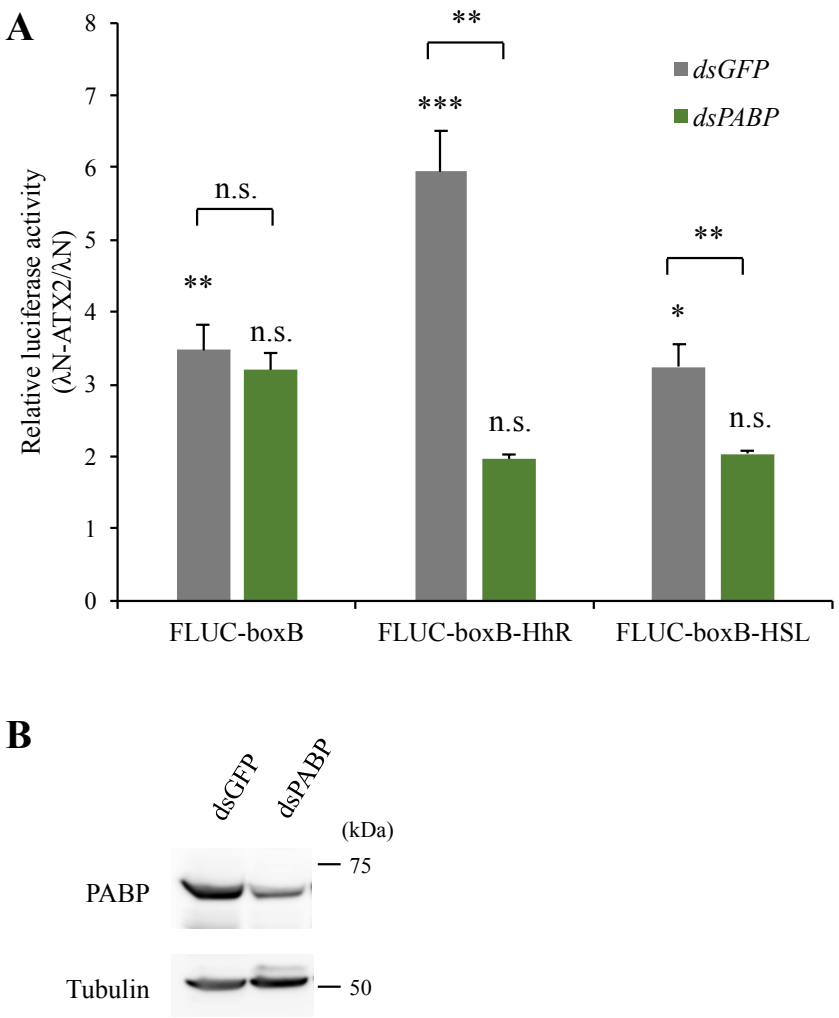

Figure III-12. PABP is necessary to activate ATX2-dependent translation

(A)PABP depletion causes de-activation of the FLUC expression by ATX2 tethering particularly at poly A-deficient reporters. S2 cell is treated with *dsGFP*(control) or *dsPABP* for each knockdown and then transfected with FLUC reporter as indicated, RLUC, and λN-tagged proteins (λN or λN-ATX2). After 48 hours from that, soluble extracts are prepared and monitored by dual luciferase assay. FLUC expression is normalized by RLUC in each samples. The relative levels are calculated by normalizing each FLUC/RLUC to λN-tethering values. Data represent mean and SEM of 3 independent experiments. n.s., not significant, $^{*}p < 0.05$, $^{**}p < 0.01$, $^{***}p < 0.001$ analyzed by one-way ANOVA, Tukey's post hoc test, compared to λN protein tethering on each indicated FLUC reporters. (B)PABP is reduced with dsRNA treatment confirmed by western blotting.

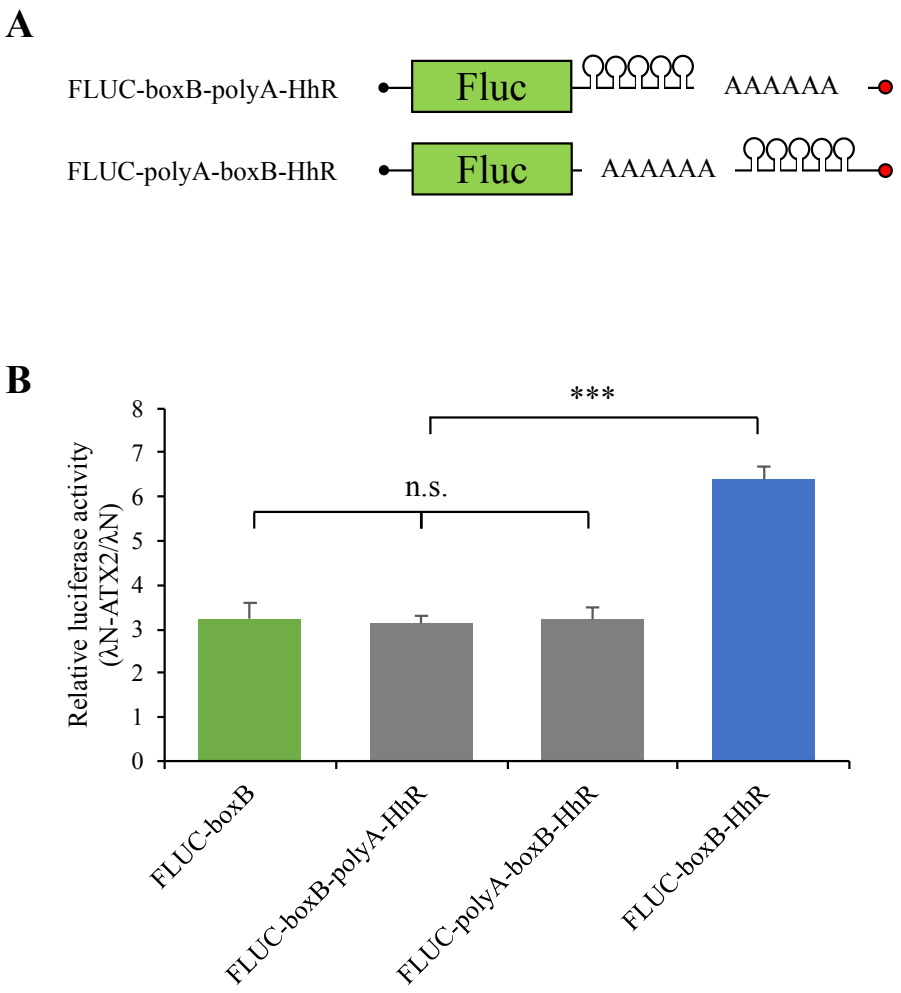

Figure III-13. HhR-specific activation by ATX2 disappears in the poly-adenylated reporters (A)Schematic structures of the reporter constructs (FLUC-boxB-polyA-HhR, FLUC-polyA-boxB-HhR). (B)Both ATX2-relevant luciferase activities in FLUC-boxB-polyA-HhR and FLUC-polyA-boxB-HhR decrease to the level of FLUC-boxB compared with FLUC-boxB-HhR. S2 cells are transfected with FLUC reporter as indicated, RLUC, and λN-tagged proteins (λN or λN-ATX2). After 48 hours from that, soluble extracts are prepared and monitored by dual luciferase assay. FLUC expression is normalized by RLUC in each samples. The relative levels are calculated by normalizing each FLUC/RLUC to λN-tethering values. Data represent mean and SEM of 4-6 independent experiments. n.s., not significant, $^{***}p < 0.001$ analyzed by one-way ANOVA, Tukey's post hoc test.

III-2-4. Repressive roles of ATX2 in 5' tethering system

PABP globally modulates translational efficiency by promoting initiation steps. In specific mRNA, PABP also represses a translation depending on its binding sites. When PABP acts on 5' UTR with repressive complex, it blocks ribosome assembly [6, 8]. To validate ATX2 effects in translation depending on its tethering sites, I changed location of boxb sequences from 3' to 5' RNA (**Figure III-14A**). In the 5' tethering system, ATX2 functions as a translational repressor on 5' end of open reading frame (ORF) (**Figure III-14B**). Unexpectedly, the repression by ATX2 is independent on PABP interaction. Also, I couldn't define a specific domain for the repression. However, deletion of N-terminal ATX2 causes partial de-repression of the activity, suggesting N-terminal ATX2 might have a function for the repression. In previous study, 5' tethering λN protein blocks ribosome scanning [27]. However, ATX2 is considered to retain specific repression mechanism since TYF (~250KD) doesn't show the repressive effect. Like ATX2, ME31B also exhibits a reduction in gene expression. There was no difference in mRNA levels depending on whether ATX2 tethering or not (**Figure III-14C**). Taken together, ATX2 on 5' end of RNA acts as a translational repressor in regardless of RNA destabilization.

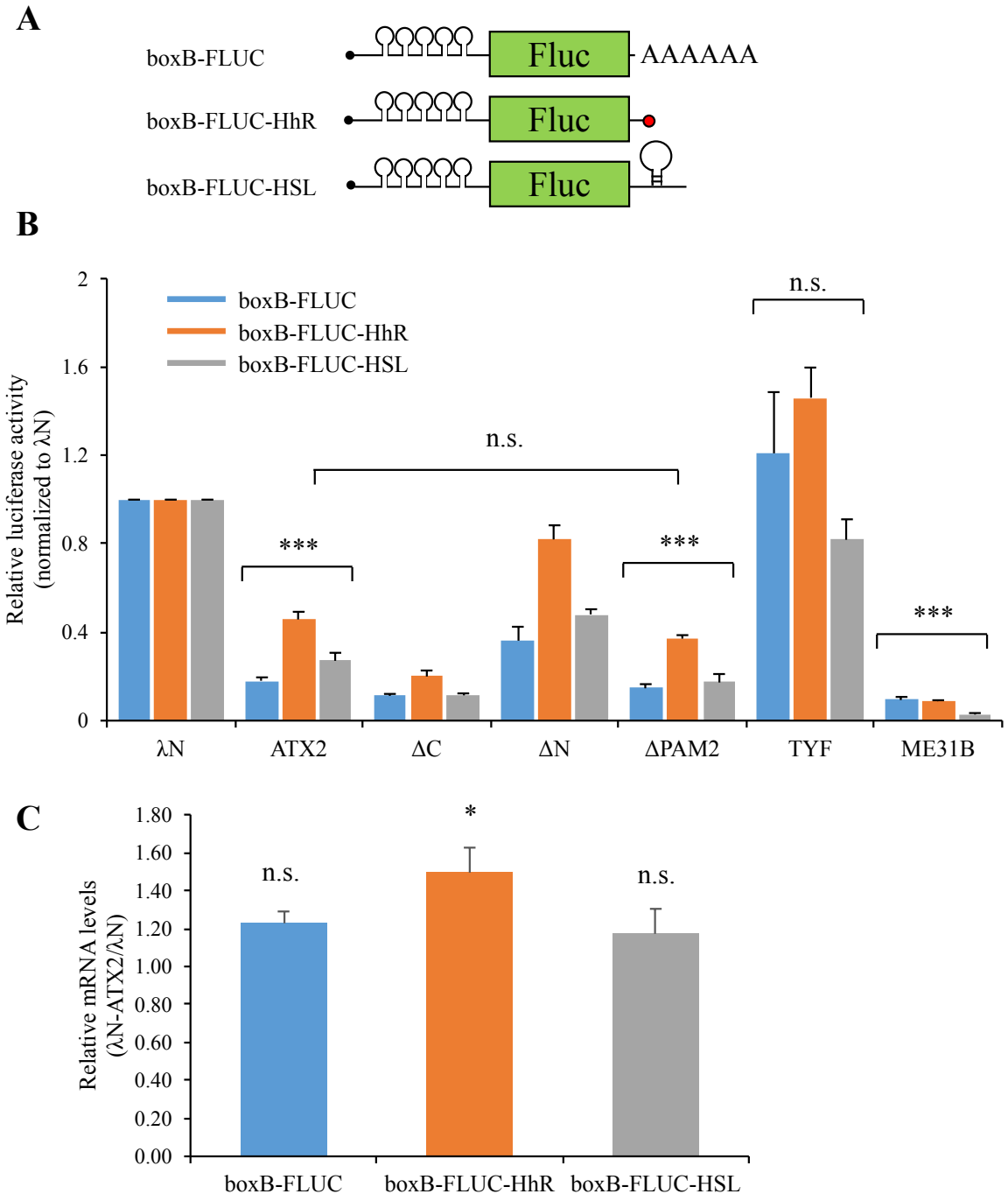

Figure III-14. ATX2 on 5' of RNA represses its expression regardless of poly A tail

(A)Schematic structures of 5' tethering reporters. As 3' tethering system, the reporters are modified with HhR or HSL. (B)5' tethered ATX2 or ME31B affects translational repression, but TYF have no effects on the translation. After transfection with FLUC reporter as indicated, RLUC, and λN-tagged proteins, soluble extracts of S2 cell are prepared and monitored by dual luciferase assay. FLUC expression is normalized by RLUC in each samples. The relative levels are calculated by normalizing each FLUC/RLUC to λN-tethering values. Data represent mean and SEM of 3-8 independent

experiments. n.s., not significant, $^{***}p < 0.001$ analyzed by one-way ANOVA, Tukey's post hoc test. (C)ATX2 on 5' of RNA has no influence on its stability. Total RNAs were prepared from transfected S2 cell with each FLUC reporter, RLUC, and λN-tagged proteins (λN or λN-ATX2). mRNA levels of FLUC is analyzed by realtime RT-PCR and normalized by RLUC in each samples. The relative levels are calculated as same way in above luciferase assay. Data represent mean and SEM of 3 independent experiments. n.s., not significant, $^{*}p < 0.05$ analyzed by one-way ANOVA, Tukey's post hoc test, compared to λN protein tethering on each indicated FLUC reporters.

III-2-5. ATX2 tethering in 5' UTR represses the translation with altered splicing

ATX2 regulates PER translation in *Drosophila* [16, 17]. Thus, I introduced *per* 5' UTR in RNA tethering system to define the translational repression in the UTR included context. The *per* 5' UTR consists of UTRs with an intron that is removed by splicing. I designed specific reporters by inserting boxB sequences into intron part of the 5' UTR (5' GTR-boxB-FLUC) or into spliced UTR part (5' UTR-boxB-FLUC) (**Figure III-15A**). As consistent with previous findings, ATX2 and ME31B tethering show repressive activities in the reporter expressions at 5' UTR (**Figure III-15B**). However, they are not affected when tethering on its intron, indicating 5' UTR-tethering ATX2 possibly controls splicing or following steps of gene expression. *Fluc* mRNA levels are slightly reduced by ATX2 or ME31B tethering but it is comparable with control group (**Figure III-15C**). In contrast, intron-tethering TYF highly activates the translation (**Figure III-15B**).

To investigate the effects on splicing by tethering each factors, I measured RNA levels targeting 5' UTR or intron with two primer sets (**Figure III-15A**). ATX2 and ME31B induce decreased transcript levels of spliced UTR, suggesting they generate damaged splicing or unstable mature mRNA in cytoplasm (**Figure III-16A**). TYF-tethering promotes splicing events in both 5' GTR and 5' UTR reporters although the protein level on 5' UTR-boxB-FLUC is similar to control (**Figure III-16B**). Taken together, 5' tethering ATX2 acts as a repressor of translation by modulating splicing or spliced mRNA stability. Therefore, different regulatory mechanisms would be manipulated depending on ATX2 binding sites.

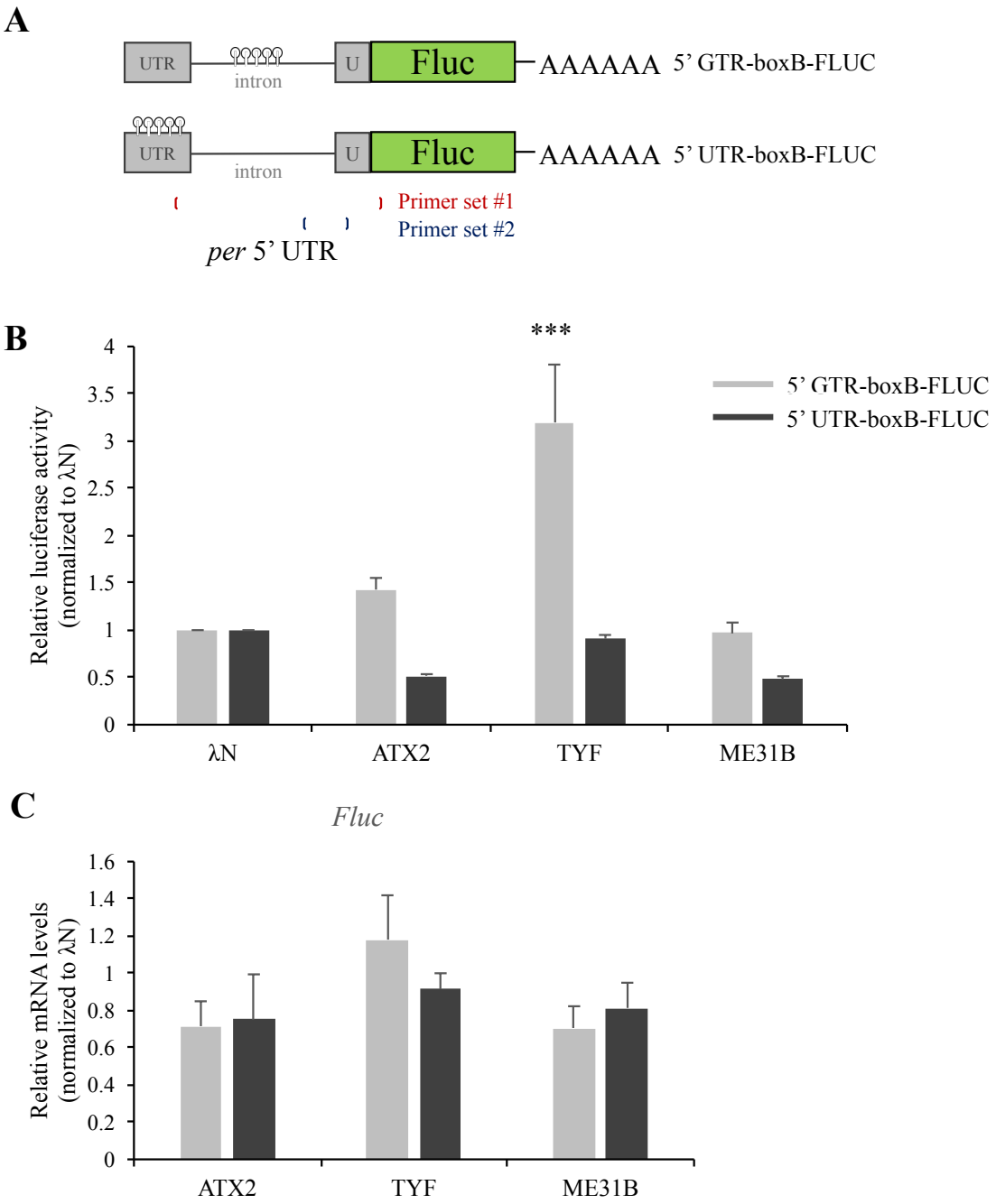

Figure III-15. ATX2 associated on 5' UTR causes translational repression

(A)Schematic structures of 5' GTR-boxB-FLUC and 5' UTR-boxB-FLUC. 5' GTR-boxB-FLUC, boxB sites in intron of 5' *per* genomic UTR (GTR); 5' UTR-boxB-FLUC, boxB sites in UTR of 5' GTR. Primer set #1 amplifies spliced UTR about 300bp in RT-PCR (or unspliced UTR about 2.6kb) and primer set #2 is for unspliced UTR including intron parts about 180bp. (B)ATX2 and ME31B on 5' UTR inhibits the gene expression. However, TYF on 5' intron activates the translation. S2 cells are transfected with FLUC reporter as indicated, RLUC, and λN-tagged proteins (λN, λN-ATX2, λN-TYF, λN-ME31B). soluble extracts are prepared and monitored by dual luciferase assay. FLUC expression

is normalized by RLUC in each samples. The relative levels are calculated by normalizing each FLUC/RLUC to λN-tethering values. Data represent mean and SEM of 3 independent experiments. $^{***}p < 0.001$ analyzed by one-way ANOVA, Tukey's post hoc test, compared to λN protein tethering on each indicated FLUC reporters. (C)The mRNA stability shows no change by each tethering proteins. Total RNAs were prepared from transfected S2 cell as indicated above. The mRNA levels of FLUC is analyzed by realtime RT-PCR and normalized by RLUC in each samples. The relative levels are calculated as same way in above luciferase assay. Data represent mean and SEM of 3 independent experiments. All results are not significant (n.s) compared to λN protein tethering on each indicated FLUC reporters.

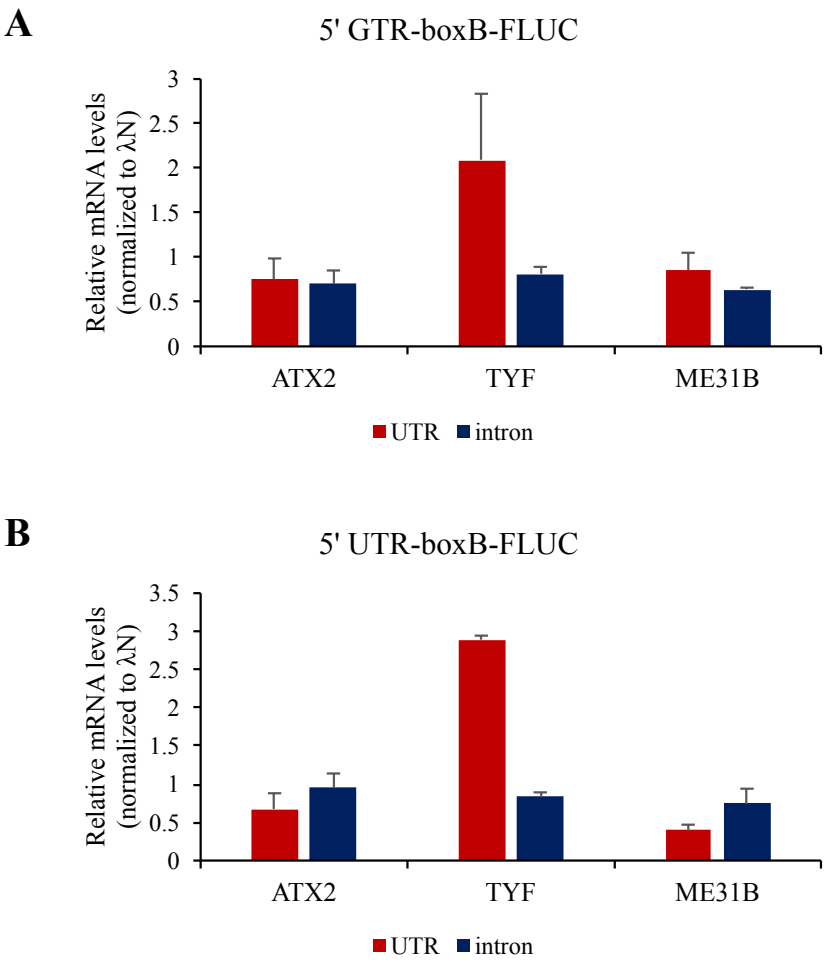

Figure III-16. ATX2 tethering in 5' UTR is implicated in RNA splicing

Abundance of each transcript including spliced or unspliced UTR by tethering ATX2, TYF, ME31B in intron of GTR (A) and UTR of GTR (B). Tethering of ATX2 and ME31B on 5' UTR affects RNA splicing. Both of TYF tethering in intron and UTR show high efficiency of the splicing. Total RNAs were prepared from transfected with each FLUC, RLUC, and λN-tagged proteins (λN, λN-ATX2, λN-TYF, λN-ME31B). The mRNA levels of FLUC is analyzed by realtime RT-PCR and normalized by RLUC in each samples. The relative levels are calculated by normalizing each FLUC/RLUC to λN-tethering values. Data represent mean and SEM of 3 independent experiments.

III-2-6. ATX2-specific activation is strongly mediated by cap-dependent manner

Overall, tethering ATX2 on the 3' end of RNA activates a translation at least in the cap-dependent context. To identify ATX2-dependent activation is globally applied or specific for cap-dependent regulation, I employed cap-independent mechanism with internal ribosomal entry sites (IRES). A RNA of Cricket Paralysis Virus (CrPV) assembles a ribosome and initiates the translation in cap-independent manner [29]. Applying IRES reporter to RNA tethering system, I designed bicistronic IRES vectors with boxb sequence (**Figure III-17A**). ATX2 tethering doesn't show IRES-dependent activation, although it acts on 3' end of transcripts (**Figure III-17B**). Even the translation slightly decreases by ATX2 tethering, suggesting ATX2-specific activation is strongly mediated by cap-dependent mechanism. In addition, I implemented cap-binding assay with wild type and PAM2 deleted mutant of ATX2 in S2 cell. Without PAM2 domain, ATX2 cannot associate with 5' cap (**Figure III-18**). Taken together, ATX2-PABP interacts with cap-binding proteins probably facilitating RNA circularization to enhance translational efficiency in only cap-dependent manner.

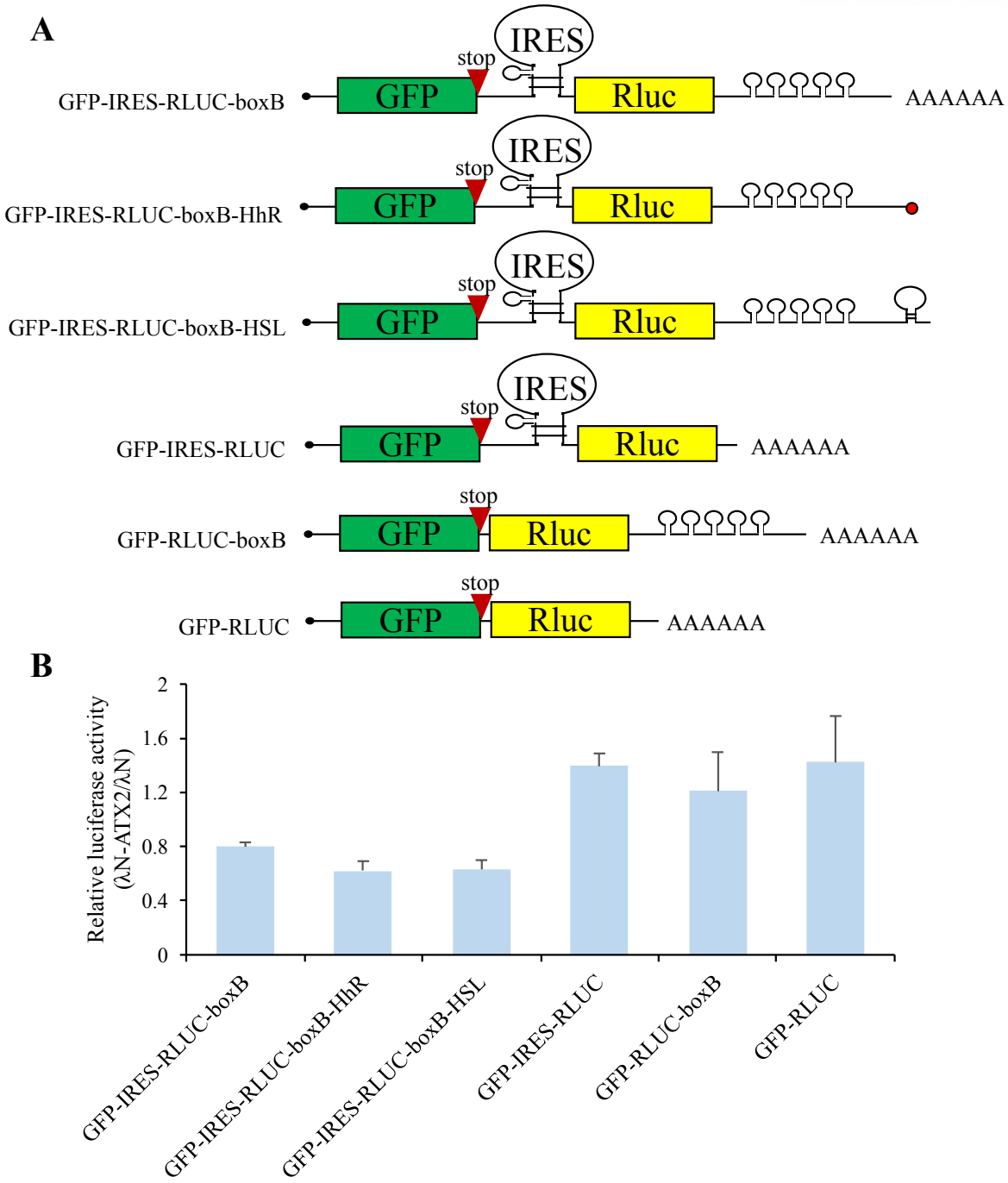

Figure III-17. ATX2 is not involved in IRES-dependent translational activation

(A)Schematic diagram of IRES reprorters. GFP coded nucleotides are located in first cistron to block cap-dependent translation of second cistron, RLUC. IRES sqeunce is derived from CrPV that induces cap-independent translation. (B)ATX2 tethering cannot activate IRES-mediate translation regardless of 3' modification. S2 cells are transfected with IRES-dependent RLUC as indicated, FLUC and λN-tagged proteins. The relative levels are calculated by normalizing each RLUC/FLUC to λN-tethering values. Data represent mean and SEM of 4 independent experiments. All results are not significant (n.s) compared to λN protein tethering on each indicated FLUC reporters.

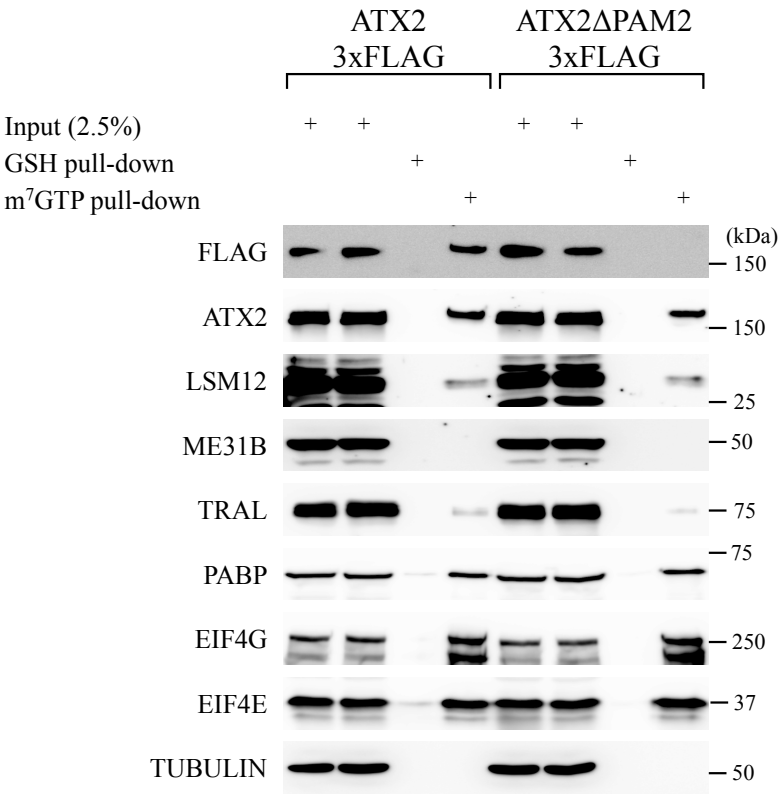

Figure III-18. PAM2 domain of ATX2 mediates 5' cap association

PAM2 deletion could not interact with 5' cap, while wild type ATX2 is detected in cap-binding complex. Soluble extracts were prepared from transfected S2 cell with the FLAG-tagged ATX2 (ATX2-3xFLAG) or PAM2 deletion (ATX2ΔPAM2-3xFLAG). The extracts are immunoprecipitated with either glutathione (GSH)- or m^7GTP-affinity beads to purify cap-binding complexes. EIF4G and EIF4E are positive controls and TUBULIN is negative controls for the cap-binding assay. Purified IP complexes were analyzed by western blotting and detected with specific antibodies (left).

IV. Discussion

IV-1. Findings of the study & corresponding models

A RNA-binding protein, *Drosophila* ATAXIN-2 (ATXN2/ATX2) acts as a post-transcriptional regulator in circadian clock [16]. I identified ATX2 forms multiple complexes with other RBPs to regulate a translation in circadian clocks (**Figure IV-1**). In ATX2-TYF dependent translational activation, LSM12 is necessary for a connection of ATX2-TYF interaction. Actually, LSM12 depletion in that complex causes de-activation of the translation suggesting all components of the complex assist the activation in circadian clock. Also, C-terminal ATX2 interacts with PABP via PAM2 domain and PABP directly binds to eIF4G [6-9]. Thus, ATX2 associates with LSM12 and TYF to 5' cap via PAM2 domain. Reversely, ME31B/DDX6 has been implicated as a translational repressor and decapping activator participating in miRNA-mediated gene silencing through CCR4-NOT deadenylase complex by direct interaction with NOT1 [35-38]. Given that ME31B doesn't interact with 5' cap and its binding complex in the result, ATX2-ME31B interaction might inhibit the translation by the dissociation of 5' cap. I demonstrated ME31B mediates NOT1 association to ATX2 supporting NOT1-dependent gene silencing. These two independent ATX2 complexes bring distinct circadian behaviors in *Drosophila* (**Figure IV-1**). Taken together, ATX2 would function as a key factor in post-transcriptional regulation to switch its associating proteins.

Although I obtained information about ATX2-associating factors on circadian clock, it remains elusive how ATX2-dependent gene expression is regulated. Thus, I examined ATX2-dependent translation with RNA-tethering assay in *Drosophila* embryo cells (S2 cells). 3' tethering ATX2 activates the gene expression depending on PAM2 domain. PABP depletion causes the de-activation of ATX2-dependent translation suggesting ATX2-PABP interaction is critical for the activation probably by RNA circularization. The tethering effect is maximized in poly A-deficient and non-circularizing itself transcripts. Taken together, I established a model for ATX2-specific activation, which ATX2 direct binding on 3' UTR of mRNA could induce mRNA circularization in short-poly A tailing transcripts instead of PABP interaction with poly A tail (**Figure IV-2**). I also elucidated an opposite role of ATX2 on 5' end of RNA as a translational repressor to decrease spliced products, indicating ATX2 has distinct mechanisms on the translation in accordance with its binding sites (**Figure IV-2**). Because ME31B shows similar activities in the 5' tethering system, ATX2 and ME31B might act together on the mechanism of translational repression. Finally, I verified ATX2 protein specifically regulates the translational activation in cap-dependent manner via PAM2 domain.

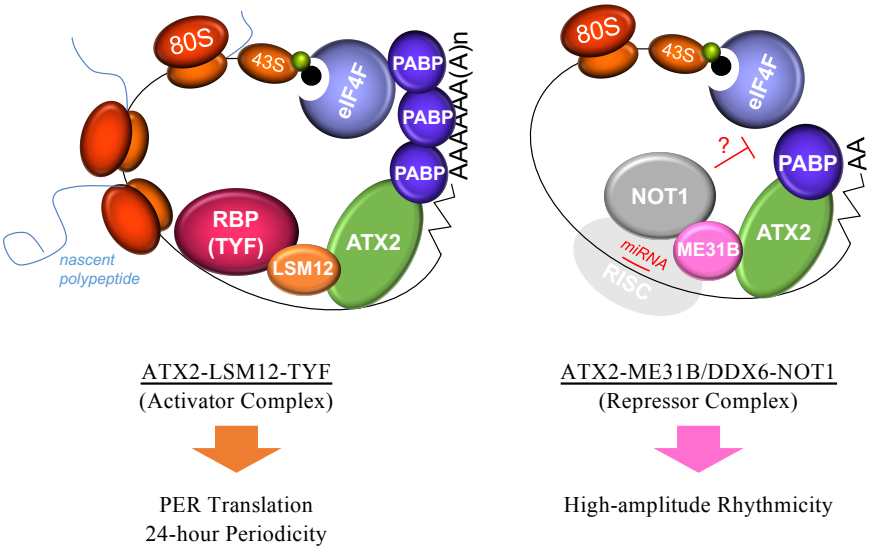

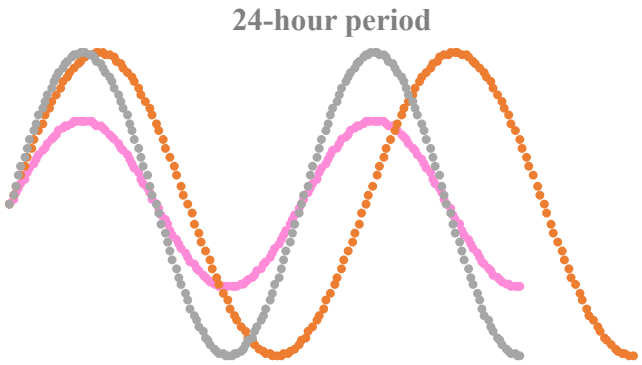

Figure IV-1. A model for post-transcriptional regulation by ATX2 with LSM12 (actvator) or ME31B (repressor) complex in circadian clocks

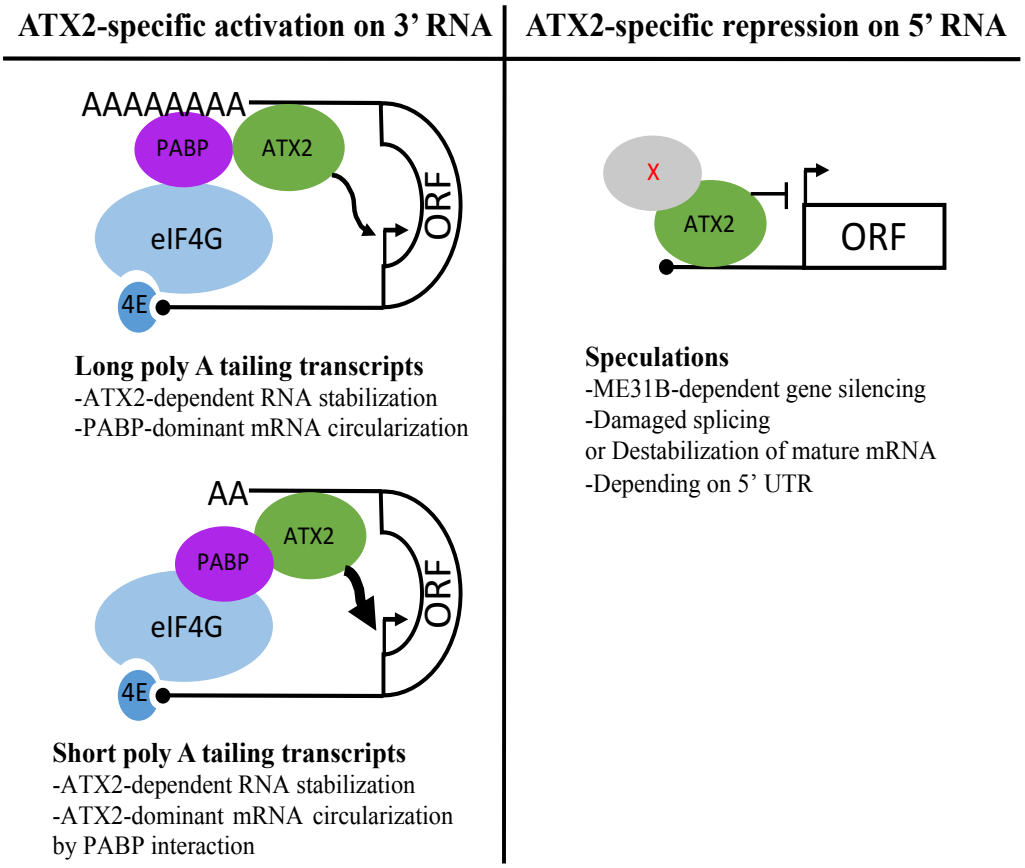

Figure IV-2. A model for ATX2-specific regulatory mechanism in mRNA translation

IV-2. Clinical implication

Drosophila ATX2 has low identity (16%), but high coverage (75%) with human ATXN2. Especially, there are two high conserved domains including N-terminal like-Sm (Lsm) domain (39% identity, 57% positive alignment) and C-terminal PAM2 (29% identity, 37% positive alignment). The identified mechanisms could be fairly applied to study ATX2-relevant disease. Actually, drosophila serve as in vivo model for human neurodegenerative disease [41].

Human spinocerebellar ataxia type 2 (SCA2) is a neurodegenerative disorder caused by CAG repeats in the ATXN2 gene and it is characterized by degeneration of Purkinje cells in the cerebellum and the progressive loss of coordination [22]. PolyQ tracts are expressed from the repeated CAG in the gene and lead to a toxic gain-of-function with ATX2 pathogenic aggregation [42, 43]. In addition, intermediate-length polyQ tracts of ATX2 is a risk factor of amyotrophic lateral sclerosis (ALS), also known as Lou Gehrig's disease [23, 24]. Actually, toxic ATX2 granules are detected in spinal cords of ALS patients [23]. These toxic ATX2 accumulations sequester its associating proteins such as

PABP into insolubility [42]. Thus, functions of ATX2-associating factors might play roles in pathogeneses of SCA2 or ALS. I discovered two additional factors, LSM12 and ME31B, in connection with post-transcriptional regulation and complicated regulatory mechanism with ATX2 as the center. By studying ATX2-interacting factors in translational regulation, ATX2-relevant pathogenic mechanism would be more accessible.

The TAR DNA-binding protein (TDP-43) was identified as a major disease protein for sporadic and familial ALS. Recent research demonstrates that ATX2 modifies TDP-43 toxicity in *Drosophila* and yeast [23]. In addition, therapeutic reduction of ataxin-2 reduces pathology in TDP-43 mice [44]. In my results, the importance of PAM2 domain for translational activation is emphasized. Given that PAM2 not only participates in mRNA stability and protein expression but also modulates TDP-43 toxicity in ALS disease model [24, 26], PAM2 could be novel domain for linkage between translational regulation and pathological pathway. Both expanded polyQ and modulation of PAM2 in ATX2 gene could induce proteome-wide changes by sequestration of associating proteins or influence on translation.

The cellular function of ATX2 is not completely characterized, but it has been suggested in regulating mRNA degradation, stability, and translation [25]. Furthermore, the loss-of-function of ATX2 affects several physiological function including obesity, insulin resistance, hyperactivity, and reduced fertility in mouse [45-47] and circadian clock and long-term memory in *Drosophila* [16, 17, 48, 49]. By elucidating ATX2 molecular function in organisms based on post-transcriptional gene regulation, I could approach to understanding of SCA2 and ALS pathogeneses.

IV-3. Further research

ATX2 has been involved in translational control under stressed condition or development [43, 50]. It indicates ATX2 regulates translation in an ‘mRNA-specific’ manner or ‘surrounding-specific’ manner. Analyses of ATX2-dependent translatome help us to obtain insights about ATX2 targets in post-transcriptional regulation. Additionally, mapping of ATX2 binding sites in the transcripts is also crucial to understand ATX2-specific mechanism. In previous study, protein association and regulatory mechanism for translational initiation are partially different depending on 5’ UTR length or structure [51]. This might explain the existence of complicated modulation by ATX2 interaction in the translation. I found ATX2 effects are differentially applied in several transcript implying ATX2 might prefer poly A-deficient or short poly A tailing transcripts to activate the translation (**Figure IV-2**). Through current technology TAIL-seq, I could easily gain information about genome wide profiling of poly A tail length of ATX2 target [52, 53]. Considering rhythmic regulation of poly A tail lengths in transcripts[10, 54], ATX2 might have specific regulatory mechanism to choose its targets depending on the poly A length and its specific activation might affect circadian behaviors.

V. References

1. Jackson, R.J., C.U. Hellen, and T.V. Pestova, *The mechanism of eukaryotic translation initiation and principles of its regulation.* Nat Rev Mol Cell Biol, 2010. **11**(2): p. 113-27.
2. Klann, E. and T.E. Dever, *Biochemical mechanisms for translational regulation in synaptic plasticity.* Nat Rev Neurosci, 2004. **5**(12): p. 931-42.
3. Reeve, B., et al., *Predicting translation initiation rates for designing synthetic biology.* Front Bioeng Biotechnol, 2014. **2**: p. 1.
4. Day, D.A. and M.F. Tuite, *Post-transcriptional gene regulatory mechanisms in eukaryotes: an overview.* J Endocrinol, 1998. **157**(3): p. 361-71.
5. Glisovic, T., et al., *RNA-binding proteins and post-transcriptional gene regulation.* FEBS Lett, 2008. **582**(14): p. 1977-86.
6. Burgess, H.M. and N.K. Gray, *mRNA-specific regulation of translation by poly(A)-binding proteins.* Biochem Soc Trans, 2010. **38**(6): p. 1517-22.
7. Kahvejian, A., et al., *Mammalian poly(A)-binding protein is a eukaryotic translation initiation factor, which acts via multiple mechanisms.* Genes Dev, 2005. **19**(1): p. 104-13.
8. Smith, R.W., T.K. Blee, and N.K. Gray, *Poly(A)-binding proteins are required for diverse biological processes in metazoans.* Biochem Soc Trans, 2014. **42**(4): p. 1229-37.
9. Sonenberg, N. and A.G. Hinnebusch, *Regulation of translation initiation in eukaryotes: mechanisms and biological targets.* Cell, 2009. **136**(4): p. 731-45.
10. Lim, C. and R. Allada, *Emerging roles for post-transcriptional regulation in circadian clocks.* Nat Neurosci, 2013. **16**(11): p. 1544-50.
11. Emery, P., et al., *CRY, a Drosophila clock and light-regulated cryptochrome, is a major contributor to circadian rhythm resetting and photosensitivity.* Cell, 1998. **95**(5): p. 669-79.
12. Price, J.L., et al., *double-time is a novel Drosophila clock gene that regulates PERIOD protein accumulation.* Cell, 1998. **94**(1): p. 83-95.
13. He, Q., et al., *Circadian Rhythm Neuropeptides in Drosophila: Signals for Normal Circadian Function and Circadian Neurodegenerative Disease.* Int J Mol Sci, 2017. **18**(4).
14. Wang, D., et al., *Ribonucleoprotein complexes that control circadian clocks.* Int J Mol Sci, 2013. **14**(5): p. 9018-36.
15. Lim, C., et al., *The novel gene twenty-four defines a critical translational step in the Drosophila clock.* Nature, 2011. **470**(7334): p. 399-403.
16. Lim, C. and R. Allada, *ATAXIN-2 activates PERIOD translation to sustain circadian rhythms*

in Drosophila. Science, 2013. **340**(6134): p. 875-9.

17. Zhang, Y., et al., *A role for Drosophila ATX2 in activation of PER translation and circadian behavior.* Science, 2013. **340**(6134): p. 879-82.
18. Ramaswami, M., J.P. Taylor, and R. Parker, *Altered ribostasis: RNA-protein granules in degenerative disorders.* Cell, 2013. **154**(4): p. 727-36.
19. Imbert, G., et al., *Cloning of the gene for spinocerebellar ataxia 2 reveals a locus with high sensitivity to expanded CAG/glutamine repeats.* Nat Genet, 1996. **14**(3): p. 285-91.
20. Pulst, S.M., et al., *Moderate expansion of a normally biallelic trinucleotide repeat in spinocerebellar ataxia type 2.* Nat Genet, 1996. **14**(3): p. 269-76.
21. Sanpei, K., et al., *Identification of the spinocerebellar ataxia type 2 gene using a direct identification of repeat expansion and cloning technique, DIRECT.* Nat Genet, 1996. **14**(3): p. 277-84.
22. Huynh, D.P., et al., *Nuclear localization or inclusion body formation of ataxin-2 are not necessary for SCA2 pathogenesis in mouse or human.* Nat Genet, 2000. **26**(1): p. 44-50.
23. Elden, A.C., et al., *Ataxin-2 intermediate-length polyglutamine expansions are associated with increased risk for ALS.* Nature, 2010. **466**(7310): p. 1069-75.
24. Kim, H.J., et al., *Therapeutic modulation of eIF2alpha phosphorylation rescues TDP-43 toxicity in amyotrophic lateral sclerosis disease models.* Nat Genet, 2014. **46**(2): p. 152-60.
25. Nonhoff, U., et al., *Ataxin-2 interacts with the DEAD/H-box RNA helicase DDX6 and interferes with P-bodies and stress granules.* Mol Biol Cell, 2007. **18**(4): p. 1385-96.
26. Yokoshi, M., et al., *Direct binding of Ataxin-2 to distinct elements in 3' UTRs promotes mRNA stability and protein expression.* Mol Cell, 2014. **55**(2): p. 186-98.
27. Eulalio, A., et al., *Deadenylation is a widespread effect of miRNA regulation.* RNA, 2009. **15**(1): p. 21-32.
28. Tritschler, F., et al., *Similar modes of interaction enable Trailer Hitch and EDC3 to associate with DCP1 and Me31B in distinct protein complexes.* Mol Cell Biol, 2008. **28**(21): p. 6695-708.
29. Majzoub, K., et al., *RACK1 controls IRES-mediated translation of viruses.* Cell, 2014. **159**(5): p. 1086-95.
30. St Johnston, D., *The art and design of genetic screens: Drosophila melanogaster.* Nat Rev Genet, 2002. **3**(3): p. 176-88.
31. Coller, J. and M. Wickens, *Tethered function assays: an adaptable approach to study RNA regulatory proteins.* Methods Enzymol, 2007. **429**: p. 299-321.
32. Behm-Ansmant, I. and E. Izaurralde, *Quality control of gene expression: a stepwise assembly pathway for the surveillance complex that triggers nonsense-mediated mRNA decay.* Genes Dev, 2006. **20**(4): p. 391-8.

33. Keryer-Bibens, C., C. Barreau, and H.B. Osborne, *Tethering of proteins to RNAs by bacteriophage proteins.* Biol Cell, 2008. **100**(2): p. 125-38.

34. Svitkin, Y.V., et al., *Eukaryotic translation initiation factor 4E availability controls the switch between cap-dependent and internal ribosomal entry site-mediated translation.* Mol Cell Biol, 2005. **25**(23): p. 10556-65.

35. Chen, Y., et al., *A DDX6-CNOT1 complex and W-binding pockets in CNOT9 reveal direct links between miRNA target recognition and silencing.* Mol Cell, 2014. **54**(5): p. 737-50.

36. Kuzuoglu-Ozturk, D., et al., *miRISC and the CCR4-NOT complex silence mRNA targets independently of 43S ribosomal scanning.* EMBO J, 2016. **35**(11): p. 1186-203.

37. Mathys, H., et al., *Structural and biochemical insights to the role of the CCR4-NOT complex and DDX6 ATPase in microRNA repression.* Mol Cell, 2014. **54**(5): p. 751-65.

38. Rouya, C., et al., *Human DDX6 effects miRNA-mediated gene silencing via direct binding to CNOT1.* RNA, 2014. **20**(9): p. 1398-409.

39. Chekulaeva, M., R. Parker, and W. Filipowicz, *The GW/WG repeats of Drosophila GW182 function as effector motifs for miRNA-mediated repression.* Nucleic Acids Res, 2010. **38**(19): p. 6673-83.

40. Zekri, L., D. Kuzuoglu-Ozturk, and E. Izaurralde, *GW182 proteins cause PABP dissociation from silenced miRNA targets in the absence of deadenylation.* EMBO J, 2013. **32**(7): p. 1052-65.

41. McGurk, L., A. Berson, and N.M. Bonini, *Drosophila as an In Vivo Model for Human Neurodegenerative Disease.* Genetics, 2015. **201**(2): p. 377-402.

42. Damrath, E., et al., *ATXN2-CAG42 sequesters PABPC1 into insolubility and induces FBXW8 in cerebellum of old ataxic knock-in mice.* PLoS Genet, 2012. **8**(8): p. e1002920.

43. Lastres-Becker, I., et al., *Mammalian ataxin-2 modulates translation control at the pre-initiation complex via PI3K/mTOR and is induced by starvation.* Biochim Biophys Acta, 2016. **1862**(9): p. 1558-69.

44. Becker, L.A., et al., *Therapeutic reduction of ataxin-2 extends lifespan and reduces pathology in TDP-43 mice.* Nature, 2017. **544**(7650): p. 367-371.

45. Huynh, D.P., et al., *Dissociated fear and spatial learning in mice with deficiency of ataxin-2.* PLoS One, 2009. **4**(7): p. e6235.

46. Kiehl, T.R., et al., *Generation and characterization of Sca2 (ataxin-2) knockout mice.* Biochem Biophys Res Commun, 2006. **339**(1): p. 17-24.

47. Lastres-Becker, I., et al., *Insulin receptor and lipid metabolism pathology in ataxin-2 knock-out mice.* Hum Mol Genet, 2008. **17**(10): p. 1465-81.

48. McCann, C., et al., *The Ataxin-2 protein is required for microRNA function and synapse-specific long-term olfactory habituation.* Proc Natl Acad Sci U S A, 2011. **108**(36): p. E655-

62.

49. Sudhakaran, I.P., et al., *FMRP and Ataxin-2 function together in long-term olfactory habituation and neuronal translational control.* Proc Natl Acad Sci U S A, 2014. **111**(1): p. E99-E108.

50. Ciosk, R., M. DePalma, and J.R. Priess, *ATX-2, the C. elegans ortholog of ataxin 2, functions in translational regulation in the germline.* Development, 2004. **131**(19): p. 4831-41.

51. Sen, N.D., et al., *eIF4B stimulates translation of long mRNAs with structured 5′ UTRs and low closed-loop potential but weak dependence on eIF4G.* Proc Natl Acad Sci U S A, 2016. **113**(38): p. 10464-72.

52. Chang, H., et al., *TAIL-seq: genome-wide determination of poly(A) tail length and 3′ end modifications.* Mol Cell, 2014. **53**(6): p. 1044-52.

53. Lim, J., et al., *mTAIL-seq reveals dynamic poly(A) tail regulation in oocyte-to-embryo development.* Genes Dev, 2016. **30**(14): p. 1671-82.

54. Kojima, S. and C.B. Green, *Analysis of circadian regulation of poly(A)-tail length.* Methods Enzymol, 2015. **551**: p. 387-403.